PAPER

Check for updates

Adsorption of semiflexible wormlike polymers to a bar and their double-chain complex formation

A. N. Semenov [ID] * and I. A. Nyrkova

We theoretically study pairing (double-strand complexation) of semiflexible wormlike chains (WLC) due to their side-to-side attraction. Considering binding of two WLCs of high stiffness we start with the case of infinite stiffness of one chain which is replaced with a straight bar. A combination of the quantitative transfer matrix approach with scaling arguments in terms of trains, loops of different sizes, tails and supertrains allowed us to characterize all the regimes of semiflexible chain adsorption on a bar. In particular, we predict a self-similar monomer concentration profile $c(r) \propto r^{-10/3}$ near the bar (at distances r below the chain Kuhn length l) at the critical point for adsorption. Such localized critical profile leads to a sharp adsorption transition. Furthermore, we found that supertrains serve as the basic structural elements in WLC complexes leading to bridging, network formation and condensation of semiflexible polymers in dilute solutions. Polymer collapse (precipitation) and redissolution on increasing attraction strength are predicted in qualitative agreement with experiments on aqueous solutions of DNA and F-actin.

1 Introduction

A semiflexible macromolecule is characterized by high stiffness of its chemical backbone: its persistence length l_p greatly exceeds its thickness d, $l_p \gg d$. On the other hand, the total contour length L of the chain can be much larger than l_p. Examples of such polymers range from Kevlar and other aromatic polyamides or synthetic polymers like derivatives of cellulose to helical polymers like poly-γ-benzyl-L-glutamate, surfactant micelles, supramolecular polymers,[1,2] self-assembling peptide tapes and fibrils,[3] and biological macromolecules like double-strand DNA, microtubules, F-actin and other protein filaments. High backbone rigidity facilitates adsorption of such polymers on solid surfaces and membranes.[4–8] On the other hand, side-to-side attraction of semiflexible macromolecules can drive their aggregation (mutual 'adsorption') leading to formation of linear double-chain or triple-chain complexes,[9,10] supramolecular fibrils and bundles.[11–16]

A similar mechanism underlies formation of polyelectrolyte complexes (PECs) in binary solutions of oppositely charged macromolecules (say, A and B).[17–23] Attraction between A and B segments has electrostatic nature in this case; it can be relatively short-range if sufficient amount of salt is added. At high polymer concentrations the two polyelectrolytes (PEs) can form complex coacervate phases,[24,25] while at low concentrations the PECs emerge as finite-size (colloidal) gel particles.[26,27] For example, chitosan, which is a semiflexible polycationic

Institut Charles Sadron, CNRS – UPR 22, Université de Strasbourg, 23 rue du Loess, BP 84047, 67034 Strasbourg Cedex 2, France

biopolymer of high stiffness, forms PECs with polyanions like polysaccharides and proteins. Such complexes play important role in biological processes and pharmaceutical applications.[26] It was also argued that highly stiff PEs should tend to form double-strand complexes in the case of strong enough attraction (Fig. 1).[17,18,28–31]

Another example of polymer complexes is provided by heteroassociative polymers bearing many functional groups (stickers) that are able to form reversible bonds (like H-bonds or metal–ligand bonds) between parallel A and B segments (Fig. 1c).[32] The transient crosslinks in associative polymer systems enable stimuli-responsiveness of their viscoelastic and rheological behavior, and numerous other remarkable dynamical and processing properties serving as a basis for many industrial and biological applications.[33–35]

In the present paper we consider complexation of semiflexible polymer chains using a rather generic and simple Kratky–Porod model (known also as worm-like chain, WLC, model) assuming that polymer conformation can be defined by its backbone trajectory and that the total interaction energy of two chains comes as a sum of short-range interactions of their length elements. The elements do not interact if their distance exceeds the interaction range Δ, $\Delta \ll l$ (here $l = 2l_p$ is Kuhn segment of the chain). Such a formally isotropic local interaction nevertheless leads to strong orientational effects due to polymer chain stiffness. The model can roughly mimic the screened Coulomb interactions of oppositely charged polyelectrolytes. It can also describe the effect of physical bonds between associating groups if the latter are sufficiently flexible, weak and numerous (many stickers per Kuhn segment).

In the next Section 2.1 we define the model in more mathematical terms and show that to a certain extent (at
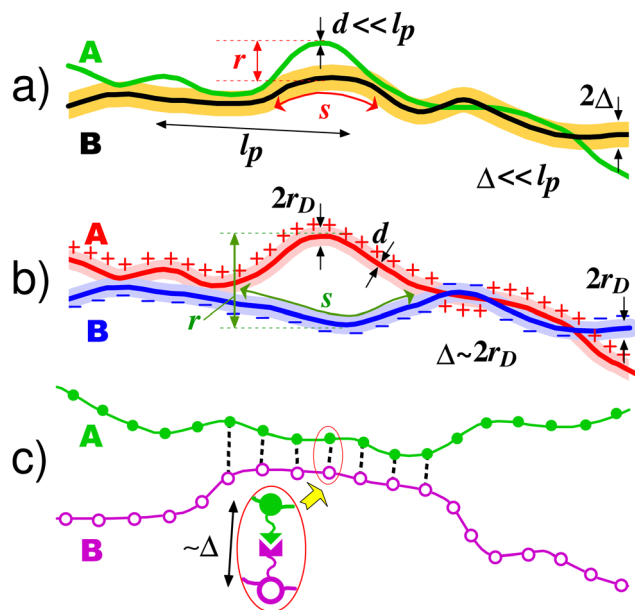
Fig. 1 Double-strand complexes of mutually attracting semiflexible chains: (a) two similar worm-like chains, A and B; Δ is the range of attractive interactions between A and B monomers (the potential well around the black chain B is shown with yellow color); d is the range of their hard-core interactions. (b) Two oppositely charged polyelectrolytes (r_D is the Debye screening length). (c) Two chains with complementary associative groups forming reversible bonds (see ladder segment in the middle). The effective rigidity of the chains is characterized by their Kuhn segment l (persistent length $l_p = l/2$); $d < \Delta \ll l$. The chain pairing (binding) is stabilized by contact regions ('trains') which alternate with 'loops'; s is the length of a loop and r is its transverse size.

length-scales shorter than l) a pairwise complexation of two WLCs is equivalent to adsorption of an effective WLC on a straight bar (standing for the second WLC in the fully stretched conformation). In Sections 2.2 and 2.3 we derive the master equation for position ($\underline{R}$) and orientation ($\underline{t}$) dependent partition function ψ of a semiflexible chain near the bar (at $r \ll l$) and obtain this function at the adsorption threshold (corresponding to the critical strength of attractive interaction, $u = u^\star$). The distribution of polymer segments in the ($\underline{R}$, $\underline{t}$)-space at $u = u^\star$ is found as well (Section 2.3). The fractal nature of this distribution is revealed using an alternative approach applied both near the bar (Sections 3.1 and 3.2) and far from it (Section 3.3). The segment distributions both below and above $u^\star$ are considered in Sections 3.4 and 3.5, respectively; the free energy of complexation is analysed in Section 3.5 as well. The main results are discussed and generalized in Section 4. We first highlight the crucial aspects of the adopted approach and the obtained results (Discussion points D1–D5), and then apply them to study the salient features of complexation between two or more semiflexible macromolecules including gelation (network formation), coil-to-globule transition and phase separation in the dilute solution regime (points D6–D9). In particular, we show that the presence of double-strand complexes can lead to a reentrant transition as solvent quality decreases (u grows): from homogeneous polymer solution to a condensed gel phase which then dissolves as the side-to-side attraction (u) gets even

stronger (see points D8, D9 of the Discussion). This effect highlights the non-trivial boundary nature of the bundling phenomenon. The results are summarized in the last Section 5.

2 Theoretical methods and basic results

2.1 The model and the theoretical problem

Below we recall some basic properties of stiff WLCs and introduce a theoretical framework to consider their pairwise complexation.

The lowest energy state of a wormlike chain (WLC) is a straight line. The free energy penalty for a deviation from this conformation is due to the chain bending:

$$F_{\text{bend}} = (Tl_p/2)\int (\mathrm{d}\underline{t}/\mathrm{d}s)^2 \mathrm{d}s = (Tl/4)\int (\mathrm{d}^2\underline{R}/\mathrm{d}s^2)^2 \mathrm{d}s \qquad (1)$$

where $\underline{t} = \underline{t}(s) = \dfrac{\mathrm{d}\underline{R}}{\mathrm{d}s}$ is unit vector tangent to the chain at point s (here s is the curvilinear distance along the chain), $\underline{R}(s)$ is position of point s, $l_p = l/2$ is the chain persistence length, and T is the thermal energy (temperature in energy units). Eqn (1) corresponds to the Kratky–Porod model,[36] which is widely used to study statistical properties of stiff and semiflexible polymer chains.[5–7,37,38] The ideal WLC model is adopted in the present study. Note that intra-chain interactions are neglected here in most cases since for $d \ll l$ the intra-chain contacts are rare.

Eqn (1) implies that at equilibrium (and in the absence of any constraints)

$$\langle \underline{t}(s+s') \cdot \underline{t}(s') \rangle = \exp(-s/l_p) \qquad (2)$$

It means that the typical bending angle of a short segment (of length $s \ll l$) is $\theta \sim (s/l)^{1/2}$, and its lateral deviation from a straight line is

$$r \sim \theta s \sim s^{3/2}/l^{1/2} \qquad (3)$$

Let us turn to the system of two WLCs, A and B, which tend to form a complex due to side-to-side attraction between A and B segments (Fig. 1a). If the attraction is sufficiently strong, the typical lateral distance r between the chains should be relatively small, $r \ll l$, so that locally the two chains have to stay nearly parallel to each other (Fig. 2a). The relevant correlation length λ along the chain can be defined by the condition that the typical lateral deviation of a λ-segment (with fixed position and orientation of its starting monomer unit) is $\sim r$: $\lambda \sim r^{2/3}l^{1/3}$ (see eqn (3)), hence $\lambda \ll l$. The paired chains can be considered as a sequence of nearly straight segments of intermediate length ΔL, $\lambda \ll \Delta L \ll l$ (see Fig. 2a). In each such segment one can choose the axis z along the chains (*cf.* Fig. 2b), so that locally the curvilinear distance s can be replaced by z-coordinate and conformations of both chains can be described by the vector functions $\underline{r}_A(z)$ and $\underline{r}_B(z)$, where $\underline{r}_i$ ($i = $ A, B) are 2-dimensional projections of position vectors onto xy plane perpendicular to z-axis. In terms of the lateral displacement vector, $\underline{r}(z) = \underline{r}_A(z) - \underline{r}_B(z)$, and the mean trajectory, $\underline{r}_m(z) = [\underline{r}_A(z) + \underline{r}_B(z)]/2$, the
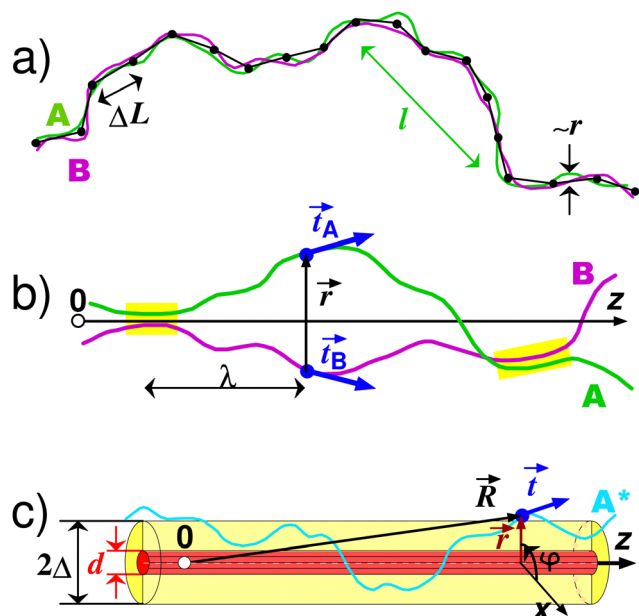
Fig. 2 The paired semiflexible chains, A (green) and B (violet) (global view (a), and local view (b)). Their mean trajectory is shown in (a) as a chain of black segments of length ΔL (only one segment of the mean chain is shown in (b) where it coincides with z-axis). l is Kuhn segment of both chains; $r \ll l$; $\lambda \sim r^{2/3}l^{1/3}$ is the relevant longitudinal correlation length; the angle θ between tangent vectors $\underline{t}_A$ and $\underline{t}_B$ is small. In (c) an effective WLC (A*, cyan) with Kuhn segment $l^* = l/2$ is adsorbed onto a straight bar of thickness d (red) with attractive zone (yellow) of radius Δ around it. The origin of the reference frame is marked in (b) and (c) with white point and sign '0'.

bending energy of both chains reads (*cf.* eqn (1) and Fig. 2):

$$F_{\text{bend}} \simeq (Tl/2)\int (d^2\underline{r}_{\text{m}}/dz^2)^2 dz + (Tl/8)\int (d^2\underline{r}/dz^2)^2 dz \quad (4)$$

Obviously the energy of local interactions between the chains depends on the lateral distance $|\underline{r}(z)|$, but is nearly independent of $\underline{r}_{\text{m}}(z)$. Hence fluctuations of $\underline{r}(z)$ and $\underline{r}_{\text{m}}(z)$ must be decoupled and therefore, as long as we are interested in the statistics of $\underline{r}(z)$, the first term in eqn (4) can be considered as irrelevant and omitted. The remaining term shows that the statistics of $\underline{r}(z)$ for two closely paired wormlike chains is equivalent to that for one WLC with effective Kuhn length $l^* = l/2$ near a straight bar attracting the WLC.† This analogy is exact in the limit $\lambda/l \to 0$ (that is, for $r \ll l$). For a finite $\lambda/l \ll 1$ the relative error of this approximation is about λ/l since the main relative inaccuracy of eqn (4) is proportional to θ^2 where $\theta \sim (\lambda/l)^{1/2}$ is the typical angle between the two chains (see the text above eqn (3) and Fig. 2b).

Thus, instead of an original complex of two tightly coupled WLCs it is appropriate to consider a simpler problem of adsorption of one effective WLC (A* with effective l^*) onto an infinite straight bar (Fig. 2c). Below we present a theoretical approach to obtain the polymer concentration distribution

---

† In the general case of different chain stiffness, l_1 and l_2, l^* is defined in eqn (106).

within the latter complex as well as its energy, free energy and other properties. Note that the problem of adsorption of a flexible (ideal Gaussian) chain onto an infinitely thin attractive bar is exactly solvable using the ground-state dominance approximation[39–41] and can be interpreted in terms of length distributions of loops and tails.[42]

2.2 The transfer-matrix approach

Let us consider an ideal semirigid WLC of length L with one end (at $s = 0$) free and the second end (at $s = L$) having orientation $\underline{t}$ and position $\underline{R} = (x, y, z)$ near a straight bar coinciding with z-axis (here s is curvilinear distance along the chain contour). In the presence of an arbitrary external potential field $U(\underline{R})$ (such that the total potential energy of the chain is $E = \int_0^L U(\underline{R}(s))ds$) the chain partition function is $\Psi = \Psi(\underline{R}, \underline{t}, L)$. This function in normalized in such a way that $\psi = 1$ in the case of no field. The obvious initial condition is then

$$\Psi(\underline{R}, \underline{t}, 0) = 1$$

Variation of Ψ as L increases can be deduced using the transfer-matrix approach[42,43] leading to the generalized Edwards equation:[5–7,43,44]

$$\frac{\partial \Psi}{\partial L} = \frac{1}{l}\nabla_{\underline{t}}^2\Psi - \underline{t}\cdot\nabla_{\underline{R}}\Psi - U(\underline{R})\Psi/T \quad (5)$$

where $\nabla_{\underline{t}}^2$ is the Laplacian in the orientational space $(\underline{t})$, and $\nabla_{\underline{R}}$ is the gradient in $\underline{R}$-space (here and below we drop '*' after l). The potential $U(\underline{R})$ is actually due to interactions between the chain and the bar. For uniform and axially isotropic bar it therefore depends only on the distance r between a short chain segment (of length ds) and z-axis: the potential energy contribution of such segment is $U(r)ds$. We assume that this interaction is short range: $U(r) = 0$ for $r > \Delta$, where Δ is much shorter than the Kuhn segment, $\Delta \ll l$. An example of $U(r)$ is shown in Fig. 3a reflecting the usual trends: attraction at r below Δ and hard-core repulsion at shorter r, $r < r_0 = d/2$; here the repulsion range r_0 is assumed to be comparable with Δ.

Eqn (5) allows to describe adsorption of the WLC on the bar. It can be rewritten using components of $\underline{t} = (t_x, t_y, t_z)$ and taking into account that the system is uniform in z-direction (since $U(\underline{R})$ is independent of z), so Ψ is also independent of z: $\Psi(\underline{R}, \underline{t}, L) = \psi(\underline{r}, \underline{t}, L)$, where $\underline{r} = (x, y)$ is the two-dimensional projection of $\underline{R}$ on the xy plane. This leads to

$$\frac{\partial \psi}{\partial L} = \frac{1}{l}\nabla_{\underline{t}}^2\psi - t_x\frac{\partial \psi}{\partial x} - t_y\frac{\partial \psi}{\partial y} - \frac{U(r)}{T}\psi \quad (6)$$
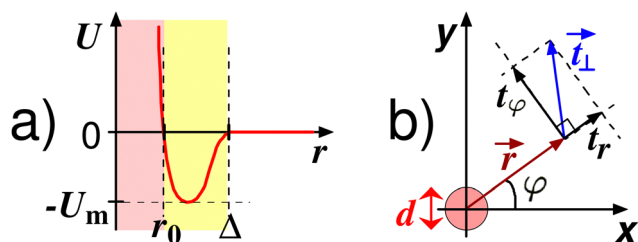
where $r = |\underline{r}|$. Furthermore, making use of cylindrical coordinates, $\underline{r} = (r\cos\varphi, r\sin\varphi)$ with polar angle φ, and defining the radial (t_r) and azimuthal (t_φ) components of the tangent vector $\underline{t}$ (*cf.* Fig. 3b),

$$t_r = t_x\cos\varphi + t_y\sin\varphi, \quad t_\varphi = t_y\cos\varphi - t_x\sin\varphi \quad (7)$$

we transform eqn (6) as

$$\frac{\partial \psi}{\partial L} = \frac{1}{l}\nabla_{\underline{t}}^2\psi - t_r\frac{\partial \psi}{\partial r} - \frac{t_\varphi}{r}\left(t_\varphi\frac{\partial \psi}{\partial t_r} - t_r\frac{\partial \psi}{\partial t_\varphi}\right) - \frac{U(r)}{T}\psi \quad (8)$$

Fig. 3 (a) The polymer/bar interaction model: $U(r)$ is interaction energy per contour length of WLC, r is the distance between a WLC element and the central axis of the bar, Δ is attraction range, $d \equiv 2r_0$ is hard-core diameter; the effective strength of the attraction can be characterized by $u = U_m/T$, $U_m \equiv |\min U(r)|$. (b) A view along the bar axis: $\underline{r}(z) = (x, y)$ is projection of the monomer position vector $\underline{R} = (x, y, z)$ onto the xy-plane (perpendicular to the bar axis z); φ is polar angle of $\underline{r}$, $x = r\cos\varphi$, $y = r\sin\varphi$; $\underline{t}_\perp$ is projection of the WLC tangent vector $\underline{t} = (t_x, t_y, t_z)$ onto the xy-plane, $\underline{t}_\perp = (t_x, t_y, 0)$; t_r and t_φ are radial and azimuthal components of $\underline{t}_\perp$ in the cylindrical coordinates (r, φ), cf. eqn (7).

where $\psi = \psi(r, t_r, t_\varphi, L)$. Here we took into account that the system is axially symmetric hence ψ is independent of the angle φ: $\left(\dfrac{\partial\psi}{\partial\varphi}\right)_{r,t_r,t_\varphi} = 0$.

For $r \ll l$ eqn (8) can be further simplified by taking into account that the chain must be nearly parallel to the z-axis due to its strong attraction to the bar (cf. the previous section), so that the tangent vector $\underline{t} = (t_r, t_\varphi, t_z)$ makes a small angle with z-axis: $|t_r| \ll 1$, $|t_\varphi| \ll 1$, $t_z \simeq 1$. As both t_r and t_φ are small, the orientational Laplacian can be written as

$$\nabla_{\underline{t}}^2 \simeq \frac{\partial^2}{\partial t_r^2} + \frac{\partial^2}{\partial t_\varphi^2} \qquad (9)$$

As a result, the master eqn (8) becomes

$$\frac{\partial\psi}{\partial L} = \frac{1}{l}\left(\frac{\partial^2\psi}{\partial t_r^2} + \frac{\partial^2\psi}{\partial t_\varphi^2}\right) - t_r\frac{\partial\psi}{\partial r}$$
$$- \frac{t_\varphi}{r}\left(t_\varphi\frac{\partial\psi}{\partial t_r} - t_r\frac{\partial\psi}{\partial t_\varphi}\right) - \frac{U(r)}{T}\psi, \quad r \ll l \qquad (10)$$

Returning to eqn (8), note that as its r.h.s. does not explicitly depend on L, its general solution can be written as a sum of terms like

$$\psi = \sum_i \psi^{(i)}(r, t_r, t_\varphi)e^{\epsilon_i L} \qquad (11)$$

where $\psi^{(i)}$, ϵ_i are eigenfunctions and eigenvalues corresponding to eqn (8). At large L the function ψ is dominated by the term with the largest $\epsilon = \max_i\{\epsilon_i\}$ corresponding to the ground-state function $\psi^{(0)}(r, t_r, t_\varphi)$ satisfying the eigenvalue equation (the superscript '0' is omitted below):

$$\frac{1}{l}\nabla_{\underline{t}}^2\psi - t_r\frac{\partial\psi}{\partial r} - \frac{t_\varphi}{r}\left(t_\varphi\frac{\partial\psi}{\partial t_r} - t_r\frac{\partial\psi}{\partial t_\varphi}\right) - \frac{U(r)}{T}\psi = \epsilon\psi \qquad (12)$$

Note that eqn (12) is valid generally, and not only for $r \ll l$. An advantage of our approach to consider a WLC near a straight bar is that the adopted approximations are valid for however

long chains (in particular, for $L \gg l$). As mentioned above the partition function of a long enough chain located near the bar is dominated by the ground state contribution (the ground-state dominance approach[39]):

$$\psi \propto e^{\epsilon L} \qquad (13)$$

At low attraction strength, $u = |\min U(r)|/T$ (see Fig. 3a), ψ does not grow with L, so $\epsilon = 0$. In this case ψ is close to the partition function of a free chain, ψ_{free}, which is constant independent of L, as follows from eqn (5) with $U(R) \equiv 0$. On the other hand, if u is sufficiently large, $u > u^\star$, the ground-state eigenvalue is positive, $\epsilon > 0$, meaning that a long chain is trapped near the bar (i.e. that the relevant solution of eqn (12) is localized, cf. Section 3.5) and its free energy per length,

$$F/L = -T\ln\psi/L \simeq -T\epsilon \qquad (14)$$

is negative. Thus, the chain is always adsorbed on the bar for $\epsilon > 0$ and the critical adsorption point (separating delocalized and adsorbed chain regimes) must correspond to $u = u^\star$ where ϵ vanishes first as u is decreased from the regime of strong attraction.

2.3 Adsorption of WLC on a bar at $\epsilon = 0$: quantitative approach for $r \ll l$

As mentioned above the chain adsorption (localization near the bar) is driven by its short-range attraction to the bar of strength u ($u = |\min U(r)|/T$, cf. Fig. 3a). Let us first focus on the critical regime (with $\epsilon = 0$, cf. eqn (12) and (14)) corresponding to the attraction threshold for the adsorption, $u = u^\star$. For $r > \Delta$ the interaction potential $U(r)$ just vanishes, so eqn (12) defining the ground-state eigenfunction $\psi(r, t_r, t_\varphi)$ can be simplified as

$$\frac{1}{l}\nabla_{\underline{t}}^2\psi - t_r\frac{\partial\psi}{\partial r} - \frac{t_\varphi}{r}\left(t_\varphi\frac{\partial\psi}{\partial t_r} - t_r\frac{\partial\psi}{\partial t_\varphi}\right) = 0 \qquad (15)$$

On using eqn (9) for $r \ll l$ we arrive at‡

$$\frac{1}{l}\left(\frac{\partial^2\psi}{\partial t_r^2} + \frac{\partial^2\psi}{\partial t_\varphi^2}\right) - t_r\frac{\partial\psi}{\partial r} - \frac{t_\varphi}{r}\left(t_\varphi\frac{\partial\psi}{\partial t_r} - t_r\frac{\partial\psi}{\partial t_\varphi}\right) = 0 \qquad (16)$$

Note that the only parameter entering eqn (16) is l, so all r-dependencies should scale with r/l. Benefiting from an analogy between adsorption onto a bar and on a flat surface,[6,7] it is natural to assume a self-similar dependence of ψ on the distance r for $l \gg r \gg \Delta$:

$$\psi(r, t_r, t_\varphi) = (r/l)^\alpha g(\eta, \xi), \qquad (17)$$

where

$$\eta \equiv t_r/\Theta(r/l), \quad \xi = t_\varphi/\Theta(r/l) \qquad (18)$$

Here the exponent α is a constant to be determined, $g(\eta, \xi)$ is a function to be found, and an appropriate function $\Theta(r/l)$ can be deduced from the structure of eqn (16) leading to:

$$\Theta(r/l) = (r/l)^{1/3} \qquad (19)$$

‡ The physical meaning of the arguments, r, t_r, t_φ, is clarified in Fig. 3b. Both t_r and t_φ are small for $r \ll l$.

Eqn (19) is in agreement with the results of ref. 6 and 7. Using eqn (16), (17) and (19) we derive the following equation for $g(\eta, \xi)$:

$$\mathcal{L}g = 0,$$

$$\mathcal{L} \equiv \frac{\partial^2}{\partial \eta^2} + \frac{\partial^2}{\partial \xi^2} + \frac{\eta}{3}\left(\eta \frac{\partial}{\partial \eta} + \xi \frac{\partial}{\partial \xi}\right) + \xi\left(\eta \frac{\partial}{\partial \xi} - \xi \frac{\partial}{\partial \eta}\right) - \alpha \eta \quad (20)$$

To solve this equation we need boundary conditions. As discussed below (cf. Section 3.5) in the adsorbed state ($u > u^*$) most segments are located close to the bar, being nearly parallel to it. If a segment of length $\lambda \ll l$ bends away from the bar, its typical deviation r from the bar and the angle θ its end makes with the bar can be estimated as $r \sim \lambda^{3/2}/l^{1/2}$, $\theta \sim (\lambda/l)^{1/2} \ll 1$ (see Section 2.1, eqn (3)). Excluding λ from these 2 equations we arrive again at eqn (19) suggesting that chain segments near the bar are aligned almost parallel to it (since $\Theta = 0$ and hence $t_r = t_\varphi = 0$ at $r/l = 0$; note that here we consider the limit $\Delta/l \to 0$). A much larger angle at a distance r, $\theta \gg \Theta(r/l)$, would require a strong bending of the λ-segment leading to a high elastic energy penalty and, therefore, low probability of such a large angle. Hence, the function $g(\eta, \xi)$ is expected to strongly decrease at large $\vartheta \equiv \sqrt{\eta^2 + \xi^2}$:§

$$g(\eta, \xi) \to 0 \quad \text{at } \vartheta \to \infty \quad (21)$$

Eqn (20) (with boundary condition, eqn (21)) could possibly be solved analytically in terms of generalized multivariable hypergeometric functions. However, we have got an impression that mathematical theory of such functions is not yet sufficiently developed.[45] So, we opted to solve eqn (20) numerically using a relaxation method. The relaxation equation associated with eqn (20) is

$$\frac{\partial g}{\partial t} = \mathcal{L}g \quad (22)$$

where t is an additional variable (fictitious time). At sufficiently long t the ground mode wins and the t-dependence readily becomes exponential, $g \propto \exp(\varkappa t)$ (compare this behavior with eqn (13)). We found that $\varkappa < 0$ for $\alpha_0 > \alpha > \alpha_1$, while $\varkappa = 0$ and therefore eqn (20) is satisfied at $\alpha = \alpha_0$ and $\alpha = \alpha_1$. The numerically obtained critical exponents are:

$$\alpha_0 = 0 \pm 5 \times 10^{-5}, \quad \alpha_1 = -2 \pm 5 \times 10^{-4} \quad (23)$$

What about the dependence of g on angular variables η and ξ in the critical states (α_0, α_1)? For $\alpha = 0$ the distribution is simply constant, $g(\eta, \xi) = $ const. However, it is non-trivial (and localized around the origin) for $\alpha \approx -2$. The typical profiles of g are shown in Fig. 4 (η-profiles (a) and ξ-profiles (b) for $\alpha = -2.0001$). Note that ξ-profiles are always symmetric, $g(\eta, \xi) = g(\eta, -\xi)$, since the system is achiral. By contrast, the η-profiles are somewhat shifted towards positive η reflecting the fact that conformations (and statistical weights ψ, cf. eqn (17)) with positive and negative t_r are not equivalent: for a given $r > \Delta$ it is more favorable to have $t_r > 0$ since in this case the end
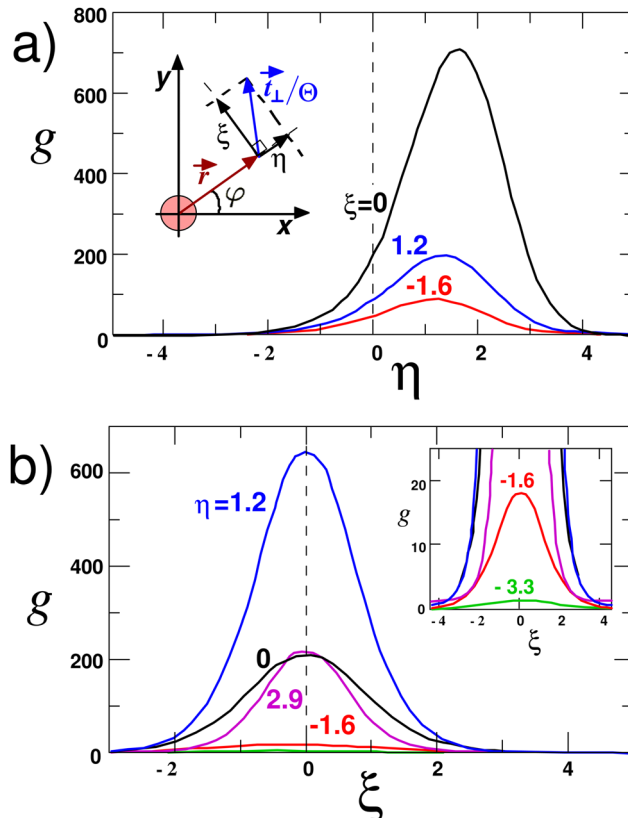
Fig. 4 The distribution of reduced angles $\eta = t_r/\Theta$, $\xi = t_\varphi/\Theta$ corresponding to the components (t_r, t_φ) of the chain-end tangent vector $\underline{t}$ in the critical regime (cf. eqn (16)–(20)): (a) $g(\eta, \xi)$ vs. η for $\xi = -1.6$ (red), 0 (black), 1.2 (blue); (b) $g(\eta, \xi)$ vs. ξ for $\eta = -3.3$ (green), -1.6 (red), 0 (black), 1.2 (blue), 2.9 (magenta).

fragment of the chain (with $s < L$ near $s = L$) is closer to the attractive bar thus increasing the probability of contacts with it.

For large ϑ the function $g(\eta, \xi)$ can be obtained analytically by a simple asymptotic analysis of eqn (20). Indeed, let us assume that $g(\eta, \xi) \simeq \tilde{g}(\vartheta) \equiv \vartheta^{-x}$ for $\vartheta \gg 1$, cf. eqn (21). Then the first term in $\mathcal{L}$, eqn (20), is negligible ($\simeq \vartheta^{-x-2}$) with respect to the second term ($\simeq \vartheta^{-x+1}$), while the third term is exactly zero for $g = \tilde{g}(\vartheta)$. The remaining second and the forth terms in $\mathcal{L}$ dictate that $x = -3\alpha$. Hence the result is

$$g(\eta, \xi) \propto \vartheta^{3\alpha}, \quad \vartheta \gg 1 \quad (24)$$

Interestingly, a similar behavior (but with different exponents α) was obtained for WLCs adsorbed onto a permeable membrane.[7]

The monomer density distribution, $c(\underline{r}, \underline{t})$, in the full space of monomer position $\underline{R}$ and orientation $\underline{t}$ is[6,7,42,43]

$$c(\underline{R}, \underline{t}) = c(r, t_r, t_\varphi) = \text{const } \psi(r, t_r, t_\varphi)\psi^\dagger(r, t_r, t_\varphi), \quad (25)$$

where $\psi^\dagger(r, t_r, t_\varphi) = \psi(r, -t_r, t_\varphi)$ is the conjugated function. The above eqn (25) is valid in the ground-state dominance (GSD) regime. Note that both ψ and c depend on just one spacial variable r (i.e. these functions are independent of both z and φ)

since the system is axially symmetric and uniform along the z-axis, *cf.* Fig. 2c. Using eqn (17) we get

$$c(r, t_r, t_\varphi) = \text{const } r^{2\alpha} g(\eta, \xi) g(-\eta, \xi) \qquad (26)$$

For large reduced angles, $\vartheta \gg 1$ (*cf.* eqn (21), *i.e.* for $t_\perp \gg \Theta(r/l)$), *cf.* Fig. 3b, we find from eqn (26) and (24) that (somewhat surprisingly) the c-function does not depend on r:

$$c(r, t_r, t_\varphi) \propto (t_r^2 + t_\varphi^2)^{3\alpha}, \quad 1 \gg t_r^2 + t_\varphi^2 \gg (r/l)^{2/3} \quad (27)$$

The significance and the physical meaning of these results are discussed in the next section.

3 Critical regimes of WLC adsorption on a bar

3.1 General concepts

As we mentioned before, the present problem of polymer adsorption on a bar is rather similar to single-chain adsorption on a flat surface. The latter phenomenon is well-studied.[6-8,46-48] For polymer adsorption (of both flexible and semirigid chains) one can distinguish two basic regimes with algebraic dependence of polymer concentration c on the distance x to the surface, $c(x) \propto x^{-\beta}$: (i) a non-adsorbed state with $\beta = \beta_0 \leq 0$ (corresponding to the case of a purely repulsive surface) and (ii) critically adsorbed state, $\beta = \beta_1 \geq 0$. The number of contacts with the surface for a chain of N units located within its own size $R \propto N^\nu$ from the surface is $n_c \propto N^\phi$, where ϕ is the so-called crossover exponent[46-48] related to β: $\phi = 1 - \nu(1 - \beta)$ if $\beta < 1$. For example, adsorption of ideal flexible chains with $\nu = 0.5$ (say, from a theta-solvent) is characterized by the critically adsorbed state with $\beta_1 = 0$, $\phi_1 = 0.5$, and the non-adsorbed state (for a repulsive wall) with $\beta_0 = -2$, $\phi_0 = -0.5$ (no polymer contacts with the surface).

Returning to adsorption of a long WLC onto a bar, the general scaling picture described above applies also in this case (with a trivial replacement of distance x with r). It is then natural and tempting to associate the exponents α_0 and α_1 (*cf.* eqn (23)) with the non-adsorbed ($u = 0$) and the critically adsorbed ($u = u^*$) states, respectively, and to check if the scaling $c \propto r^{-\beta}$ holds. To obtain $c(r)$, eqn (26) must be integrated over the 'angles' t_r and t_φ. For $\alpha = \alpha_0 = 0$ the result is $c(r) \propto r^\alpha = \text{const}$, hence $\beta_0 = 0$. (Note that the angular factor $g(\eta, \xi)$ for $\alpha = 0$ is not only constant asymptotically, but it is also identically constant: $g = \text{const}$ is the exact solution of eqn (20) and (15) in this case.)¶ By contrast, the angular integration in eqn (26) for $\alpha = \alpha_1 = -2$ provides an important factor

$$\int g(\eta, \xi) g(-\eta, \xi) \mathrm{d}t_r \mathrm{d}t_\varphi \sim r^{2/3} \qquad (28)$$

(*cf.* eqn (18) and (19)) leading to the critical exponent $\beta_1 = 10/3$:

¶ Therefore $\alpha_0 = 0$ is an exact result. Moreover, $\alpha_1 = -2$ also rigorously comes from eqn (20), $\mathcal{L}g = 0$, where the operator $\mathcal{L} = \mathcal{L}(\alpha)$ depends on the parameter α. The reason is that the operators $\mathcal{L}(0)$ and $\mathcal{L}(-2)$ have exactly the same eigenvalue spectrum since, as follows from the definition of $\mathcal{L}$, the second eqn (20), $\mathcal{L}(-2)$ equals to $\mathcal{L}^\dagger(0)$ with variable η replaced by $-\eta$, where $\mathcal{L}^\dagger$ is the transpose of $\mathcal{L}$ (being real, $\mathcal{L}^\dagger$ is also conjugated to $\mathcal{L}$).

$$c(r) \propto r^{2\alpha + 2/3} = r^{-10/3} \qquad (29)$$

Below we present an alternative derivation of the above law based on a scaling argument.

3.2 Self-similar structure of loops in the proximal layer at $u = u^*$

To begin with let us estimate the attraction strength threshold u^* for the critical adsorption of a long WLC ($L \gg l$). To fully benefit from attraction to the bar (*cf.* Fig. 3a) a chain segment of length λ should be located in the attraction region $r < \Delta$. The entropic cost for such confinement is ~ 1 per segment of length λ^* whose lateral displacement r is small, $r \lesssim \Delta$. Using eqn (3) we get

$$\lambda^* \sim (\Delta^2 l)^{1/3} \qquad (30)$$

The energy gain (in units of thermal energy T) due to attraction of a λ^*-segment to the bar is $u\lambda^*$, so the attraction gain dominates the entropy loss if $u\lambda^* \gtrsim 1$. Hence, the WLC adsorption is favorable for

$$u > u^* \sim (\Delta^2 l)^{-1/3} \qquad (31)$$

An analogous scaling argument was used before to obtain a similar estimate of u^* for adsorption on a flat solid surface or a membrane.[5-7,49]

The typical angle θ^* between the tangent vector of an adsorbed λ^*-segment of the WLC and the bar is small:

$$\theta^* \sim (\lambda^*/l)^{1/2} \sim (\Delta/l)^{1/3} \qquad (32)$$

Such a segment is called a 'train' below (*cf.* Fig. 5).

Considering the critical point $u = u^*$, we note that the free energies of adsorbed and non-adsorbed chains must be balanced since $\epsilon = 0$ at this point. Therefore, the typical conformation of a long critically adsorbed chain should include 'loops' of different sizes in addition to 'trains' (see Fig. 5). Note that the attraction energy of one train is $E_{\text{train}} \simeq Tu^*\lambda^* \sim T$. The partition function of a loop of length $s \gg \lambda^*$ is $Z_l(s)$. To find it we recall that the lateral size of such a loop is (*cf.* eqn (3))

$$r(s) \sim s^{3/2}/l^{1/2}, \qquad (33)$$

so the fraction f_Δ of its segments in the Δ-region is negligible, $f_\Delta \sim \Delta^2/r(s)^2 \sim (\lambda^*/s)^3 \ll 1$ and $f_\Delta s \ll \lambda^*$, so its interaction energy E with the bar is small, $E \ll E_{\text{train}} \sim T$. Therefore, the loop can be considered as a virtually free fragment with the only condition that its second end must be near the bar and oriented nearly parallel to it (within the angle $\sim \theta^*$). The corresponding probability, $p_{\text{loop}} \sim (\Delta/r(s))^2(\theta^*/\theta(s))^2$, where $\theta(s) \sim (s/l)^{1/2}$, provides the partition function of a loop of length s:

$$Z_l(s) = p_{\text{loop}} \sim (\lambda^*/s)^4 \qquad (34)$$

The number $N(s)$ of such loops with length equal exactly to s is proportional to $Z_l(s)$ since any chain fragment can form a loop with probability p_{loop}. Hence the number of monomer units in all loops of size $\sim s$ (say, between $s/2$ and s) is $\mathcal{N}(s) \propto s^2 Z_l(s)$. Most of these monomers are located at the distance $\sim r(s)$ from the bar, the corresponding area in the transverse (xy) plane is
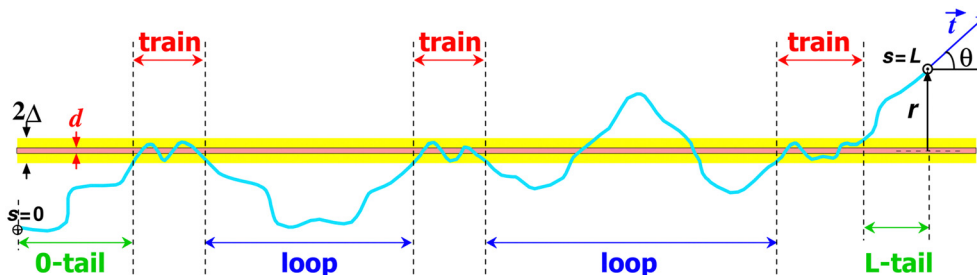
Fig. 5 Polymer chain adsorbed onto a bar: trains, loops and tails. Train is a chain section located near the bar (at $r \lesssim \Delta$) which is locally directed along the bar ($\theta \lesssim \theta^\star \sim (\Delta/l)^{1/3}$); loop is a chain fragment between two trains; 0-tail is the chain section between the left end and the first train, L-tail is the section between the last train and the right end.

$A(s) \sim r(s)^2$. Therefore, polymer concentration at $r \sim r(s)$ is $c \propto \mathcal{N}(s)/A(s) \propto 1/(s^2 r^2)$. Recalling eqn (33) we thus get

$$c(r) \propto r^{-10/3} \quad \text{for } l \gg r \gg \Delta \qquad (35)$$

in agreement with eqn (29). This way we not only justify the transfer matrix approach (Sections 2.2 and 2.3), but also show that the critical exponent $\alpha = \alpha_1$ (*cf.* eqn (23)) must be exactly equal to -2. A similar argument to get the critical exponent was proposed for a WLC near an attractive membrane.[6,7] ∥

It is natural to expect that $c(r)$ is roughly constant at $r_0 < r \sim \Delta$. Therefore, a significant fraction $p(\Delta,l)$ of polymer (in the region $r \lesssim l$ where the chain stiffness does matter)

$$p(\Delta, l) = \int_0^\Delta c(r) r\, \mathrm{d}r \Big/ \int_0^l c(r) r\, \mathrm{d}r \qquad (36)$$

is concentrated in the Δ-region near the bar: $p(\Delta,l) \sim 1/2$ since $\int_0^l c(r) r\, \mathrm{d}r$ is dominated by the contribution from $r \sim \Delta$. The above argument shows that at the critical adsorption point, $u = u^\star$, the adsorbed structure in the proximal region $\Delta < r < l$ can be viewed as a system of loops with fractal size distribution (*cf.* eqn (34) and (35)). A similar conclusion was drawn for adsorption of WLCs onto membranes.[6,7]

3.3 Distal layer

Let us turn to the adsorption regime above the critical point, $u \geq u^\star$, where $\epsilon \geq 0$. At $r \gg l$ a long WLC (with $L \gg l$) can form a distal layer in addition to the proximal (cylindrical) layer at $l \gg r > \Delta$ studied in the previous section. In the distal zone ($r \gg l$) the chain rigidity does not matter and, hence, the angular dependence of the partition function ψ can be neglected: $\psi(\underline{r}, \underline{t}) \simeq \psi(\underline{r})$, where $\psi(\underline{r})$ satisfies (in the GSD approximation valid for $L \to \infty$)** the classical equation for ideal flexible polymers:[6,7]

$$\frac{l}{6} \nabla_{\underline{r}}^2 \psi = \epsilon \psi \qquad (37)$$

∥ Note that the scaling law of eqn (34) is asymptotically valid for short loops of length s, $\lambda^\star \ll s \ll l$. Furthermore, eqn (35), which follows from eqn (34), defines the contribution of such loops to the concentration profile. No logarithmic prefactors are omitted in these equations; small (vanishing) corrections to these scaling laws decay algebraically rather than logarithmically.

** Note that in the general case $\psi(\underline{r})$ is defined in eqn (42).

Here $\nabla_{\underline{r}}^2$ is Laplacian in the xy plane, $\underline{r} = (x, y)$. For axially symmetric ground state $\psi = \psi(r)$ and $\nabla_{\underline{r}}^2 \psi = \frac{1}{r} \frac{\partial}{\partial r}\left(r \frac{\partial \psi}{\partial r} \right)$. Hence for $\epsilon > 0$ the only solution of eqn (37) that does not increase exponentially at $r \to \infty$ is

$$\psi(r) = \text{const } K_0(r/h), \quad h = \sqrt{l/(6\epsilon)} \qquad (38)$$

where h is the terminal size of the layer, and K_0 is the MacDonald function. Using $K_0(z) \simeq \ln(1/z)$ at $z \ll 1$, we find for $r/h \ll 1$:

$$\psi(r) \simeq \text{const } \ln(h/r), \quad h \gg r \gg l \qquad (39)$$

At the adsorption threshold $u - u^\star = 0^+$ the adsorption free energy vanishes ($\epsilon = 0^+$) formally implying that $h \to \infty$. To avoid this singularity (which simply means that at $u \leq u^\star$ the chain can go away from the bar) we restrict the chain conformational space by demanding that the chain end is located not farther than the coil size, R_{coil}, from the bar: $r < R_{\text{coil}}$ (here $R_{\text{coil}} = \sqrt{Ll}$ for $L \gg l$). This condition implies that if h is larger than R_{coil}, it must be replaced with R_{coil} in eqn (39).

Let us now consider the subcritical regime, $u < u^\star$. As discussed in point D2 of Section 4, at $u = 0$ the function $\psi = \psi(\underline{r}, \underline{t})$ is nearly independent of both position $\underline{r}$ and orientation $\underline{t}$ in the distal region, $r \gg l$ (*i.e.* the presence of the bar does not affect ψ in this region). On using eqn (25) we find that the same is true for the concentration distribution:

$$c(\underline{r}, \underline{t}) = c(r, t_r, t_\varphi) \simeq \text{const}, \quad r \gg l, \quad u = 0 \qquad (40)$$

We are now ready to describe the functions $\psi(\underline{r}, \underline{t})$ and $c(\underline{r}, \underline{t})$ for both critically adsorbed ($u = u^\star$, $\psi = \psi_1$ with $\alpha = \alpha_1$, see eqn (23)) and non-adsorbed ($u = 0$, $\psi = \psi_0$ with $\alpha = \alpha_0$) states. Using eqn (24), (17) and (39) with $\alpha = \alpha_1 = -2$ and assuming a smooth crossover between proximal and distal regimes (see point D4 of Section 4 for a more detailed discussion) we get $\psi = \psi_1$ at $u = u^\star$:

$$\psi_1(\underline{r}, \underline{t}) \sim \begin{cases} \theta^{-6}, & \Delta \ll r \ll l, \theta \gtrsim (r/l)^{1/3} \\ (l/r)^2, & \Delta \ll r \ll l, \theta \lesssim (r/l)^{1/3} \\ \ln(h/r), & l \lesssim r \ll h \end{cases} \qquad (41)$$

where $h = R_{coil}$ and $\theta \simeq \sqrt{t_r{}^2 + t_\varphi{}^2}$ is the angle between the tangent vector $\underline{t}$ (of the chain end) and z-axis. ††

The position-dependent partition function $\psi(\underline{r})$ results from orientational averaging of $\psi(\underline{r}, \underline{t})$:

$$\psi(\underline{r}) = \int \psi(\underline{r}, \underline{t}) \mathrm{d}^2 t / (4\pi) \tag{42}$$

where $\mathrm{d}^2 t$ is the steric angle element. Using eqn (41) we find

$$\psi_1(r) \sim (l/r)^{4/3}, \quad \Delta \lesssim r \ll l \tag{43}$$

in the proximal region, and

$$\psi_1(r) \sim \ln(h/r) \quad \text{for } h \gg r \gtrsim l \tag{44}$$

in the distal region (see also Discussion point D4).

Turning to the distribution $c(\underline{r}, \underline{t})$ at $u = u^*$, it is approximately given by $c(\underline{r}, \underline{t}) \sim \text{const}\, \psi(\underline{r}, \underline{t})^2$ (cf. eqn (25) and (41) and note an agreement of the resultant $c(\underline{r}, \underline{t})$ with eqn (27) for the proximal regime). Integrating $c(\underline{r}, \underline{t})$ over orientations we get (using eqn (41))

$$c(r) \sim c_0 \cdot \begin{cases} (r/l)^{-10/3}, & \Delta \ll r \ll l \\ \ln^2(h/r), & h \gg r \gtrsim l \end{cases} \tag{45}$$

where c_0 is a constant. Eqn (45) is in agreement with eqn (29) for $\alpha = -2$ (see also Discussion point D3).

The functions $\psi = \psi_0(\underline{r}, \underline{t})$ and $c(r)$ for the non-trapped case, $u = 0$, $\alpha = \alpha_0 = 0$, can be obtained in a similar way. Using eqn (24), (17) and (40) we get:

$$\psi_0(\underline{r}, \underline{t}) \simeq 1, \quad c(r) \sim c_0, \quad \Delta \ll r \lesssim h \tag{46}$$

in agreement with conclusions drawn above eqn (28) (see also point D2 of Section 4).

3.4 Concentration profile below the critical point, at $0 < u < u^*$

The natural next question is how the functions ψ and c evolve as u is decreased from u^* to the athermal point $u = 0$, that is, for any τ, $0 < \tau < 1$, where

$$\tau \equiv (u^* - u)/u^* \tag{47}$$

measures the deviation from the critical point. Here it is important to note that both limiting functions, $\psi = \psi_0$ (for $u = 0$) and $\psi = \psi_1$ (for $u = u^*$), satisfy the same master eqn (15) outside the bar, in the region $r > \Delta$ where $U(r) \equiv 0$. Although, strictly speaking, the general solution of eqn (15) in this region

is a linear combination of an infinite spectrum of independent ψ-functions, the two functions, ψ_0 and ψ_1, play a special role below the critical point ($u < u^*$) as stated in ref. 6: the actual solution, ψ, of eqn (15) in this regime can be approximated as a linear combination of the two basic functions, $\psi(\underline{r}, \underline{t}) = \frac{1}{1 + C}[\psi_1(\underline{r}, \underline{t}) + C\psi_0(\underline{r}, \underline{t})]$, where $C = C(\tau)$ is defined by the effective boundary condition at $r = \Delta$ (i.e. at the boundary of the region where eqn (15) applies) which, in turn, is defined by the potential $U(r)$ in the interaction zone $r < \Delta$. ‡‡ It is natural to assume that C is linear in the potential strength u, and therefore is proportional to the deviation τ from the critical value:

$$C \simeq k\tau, \quad \tau \ll 1$$

Thus

$$\psi(\underline{r}, \underline{t}) \simeq \psi_0(\underline{r}, \underline{t}) + \frac{1}{1 + k\tau}\psi'(\underline{r}, \underline{t}) \tag{48}$$

where

$$\psi'(\underline{r}, \underline{t}) \equiv \psi_1(\underline{r}, \underline{t}) - \psi_0(\underline{r}, \underline{t}) \tag{49}$$

$\psi_1(\underline{r}, \underline{t})$ is partition function for critical adsorption, and $\psi_0(\underline{r}, \underline{t}) \simeq 1$ is the contribution of non-adsorbed chain conformations which do not involve any trains, cf. eqn (46). (As argued in point D2 of Section 4, ψ_0 is not affected by the presence of the bar under weak conditions specified there.) The parameter k is important; it is calculated using a different approach (which also validates eqn (48) at $0 < \tau \leq 1$) in point D5 of Section 4: $k \sim (l/\Delta)^2$. From eqn (48) it is then clear that $\psi \simeq \psi_1$ at low $\tau \ll \tau_c$ where

$$\tau_c \equiv 1/k \sim (\Delta/l)^2 \tag{50}$$

At $\tau \sim \tau_c$ the function ψ is roughly an arithmetic average of ψ_0 and ψ_1 and therefore ψ is dominated by the critical contribution ψ_1 since $\psi_1 \gg \psi_0$ at $r \ll h$ (cp. eqn (41) and (46)). A similar domination applies to the concentration profile $c(r)$ at $\tau \lesssim \tau_c$. Thus, in this regime both $\psi(r,t)$ and $c(r)$ are approximately defined by eqn (41) and (45) and the critical self-similar structure of loops for $r \ll l$ (described in Section 3.2) stays intact.

For $\tau \gg \tau_c$ the end-partition function is isotropic for $r \gtrsim \Lambda \equiv \tau^{-1/2}\Delta$ (note that $\Lambda \sim l(\tau_c/\tau)^{1/2} \ll l$ in this regime):

$$\psi \simeq 1 + (\tau_c/\tau) \cdot \begin{cases} \ln(h/r), & h \gtrsim r \gtrsim l \\ \ln(h/l), & l \gtrsim r \gtrsim \Lambda \end{cases} \tag{51}$$

as follows from eqn (41), (46), (48) and (49). (Note that $h = R_{coil}$ for $u \leq u^*$.) The behavior of ψ at shorter distances, $\Delta \ll r \ll \Lambda$,

---

†† Note that $\psi_1 \sim 1$ for $r \sim h$. This feature can be also deduced from the fact that the chain behaves 'flexibly' at $r \gg l$, hence the results for flexible chains in the presence of a localized attractive potential are applicable.[42] More precisely, we can solve eqn (5) in the form of eqn (11): $\psi(\underline{R}, \underline{t}, L) = \sum \psi^{(i)}(\underline{R}, \underline{t}) \exp(\varepsilon_i L)$, and note that $\psi^{(0)}(\underline{R}, -\underline{t})$ is orthogonal to all $\psi^{(i)}(\underline{R}, \underline{t})$ with $i > 0$ (the latter statement is a generalization of a well-known fact that eigenvectors of a Hermitian operator are mutually orthogonal). Noting also that $\psi(\underline{R}, \underline{t}, 0) = 1$ and that $\psi^{(0)}$ and $\varepsilon^{(0)}$ must correspond to $\psi^{(0)} \simeq \psi_1(r)$ (at $r \gg l$), and $\varepsilon^{(0)} = 0^+$ at the critical point, we get

$$\int \psi_1(r) \mathrm{d}^2 r \simeq \int \psi_1(r)^2 \mathrm{d}^2 r$$

Eqn (39) suggests that both integrals above are dominated by the region $r \sim h$, so the above equation demands that const in eqn (39) is nearly equal to 1.

---

‡‡ The prefactor $\frac{1}{1 + C}$ here comes from the notion that $\psi \sim 1$ at $r \sim h = R_{coil}$ for any $u \leq u^*$: this is obviously true for $u = u^*$ (see the last line in eqn (41)), and for $u = 0$. Note that while $\psi \simeq 1$ in the latter case ($u = 0$) comes from eqn (46), it can be also deduced from the fact that the probability that any segment of the chain (whose end is located at a distance $r \sim h = R_{coil}$ from the bar) comes close to the bar (within a distance $\sim l$) is logarithmically small as follows from the Gaussian (flexible chain) statistics which is applicable in this case since all relevant length-scales here are larger than the persistence length $l_p = l/2$.

is described below based on eqn (48), (41) and (46):

$$
\psi \sim
\begin{cases}
(\tau_c/\tau)(l/r)^2, & r \ll \Lambda, \quad \theta \lesssim (r/l)^{1/3} \\
(\tau_c/\tau)\theta^{-6}, & r \ll \Lambda, \quad (r/l)^{1/3} \lesssim \theta \lesssim (\tau_c/\tau)^{1/6} \\
1 + (\tau_c/\tau)\ln(h/l), & r \ll \Lambda, \quad \theta \gtrsim (\tau_c/\tau)^{1/6}
\end{cases}
\tag{52}
$$

The monomer density distribution in the $(\underline{r}, \underline{t})$ space is $c(\underline{r}, \underline{t}) \sim \text{const}\,\psi(\underline{r}, \underline{t})^2$ (see text above eqn (45)). Integrating over orientations $\underline{t}$ we get the concentration profile (a constant common prefactor is omitted):

$$
c(r) \sim \left(\frac{l}{r}\right)^{10/3} + \ln^2(h/r) + \left(\frac{\tau}{\tau_c}\right)^2
\tag{53}
$$

where $h = R_{\text{coil}}$. Obviously, the total concentration profile reflects the adsorbed self-similar structure at short r (cf. eqn (29)) and isotropic non-adsorbed virtually free state (corresponding to the last term in eqn (53)) at larger distances (cf. eqn (46)). The polymer concentration strongly increases at short r. The proximal fractal region of aligned loops is preserved, but gets thinner at $\tau \gg \tau_c$: $c(r) \propto r^{-10/3}$ is valid only for $\Delta \ll r \ll l(\tau_c/\tau)^{3/5} \ll \Lambda$, where $\Lambda = \tau^{-1/2}\Delta \ll l$.

Eqn (53) also shows that for $\tau \lesssim \tau_c = (\Delta/l)^2$ the polymer mass in a cylindrical region of radius $r^* \sim l(l/\Delta)^{2/3}$ well-exceeding l, $r^* \gg l$, is dominated by the adsorbed segments located very close to the bar, at $r \lesssim \Delta$.

3.5 Concentration profile above the adsorption threshold, $u > u^\star$ ($\tau < 0$)

In the adsorption regime, $u > u^\star$ (where $\tau < 0$) the chain gets trapped in a region $r \lesssim h$ near the bar. The localization length h depends on u but is independent of the chain length L if it is long enough ($R_{\text{coil}} \gg h$). The cut-off length h is related to the adsorption free energy per length, ϵT, which is positive for $u > u^\star$. In the regime of long chains, $\epsilon L \gg 1$, considered below the WLC is really trapped near the bar, so the chain can be considered basically as a sequence of loops and trains (cf. Fig. 5). While at $u = u^\star$ loops of any size are allowed, at $u > u^\star$ a loop of length s costs the free energy $\Delta F(s) \simeq s\epsilon T$ which is the penalty for desorption of an s-segment from the bar (cf. ref. 6, 7 and eqn (14)), so the statistical weight of a loop, eqn (34), is reduced by the Boltzmann factor $\mathrm{e}^{-\Delta F(s)/T} \simeq \mathrm{e}^{-\epsilon s}$ suppressing the loops of length $s \gg 1/\epsilon$. The cut-off length $h = h(\epsilon)$ can be estimated as the lateral size r_1 of the largest loops of length $s = s_m \sim 1/\epsilon$ (the size of its projection onto the xy plane). This size depends on s according to eqn (33) at $s \lesssim l$, and shows the standard Gaussian chain behavior in the semiflexible regime, $s \gg l$:

$$
r_l(s) \sim
\begin{cases}
s^{3/2}l^{-1/2}, & s \lesssim l \\
\sqrt{sl}, & s \gtrsim l
\end{cases}
\tag{54}
$$

Therefore

$$
h \simeq
\begin{cases}
\dfrac{3}{16}\epsilon^{-3/2}l^{-1/2}, & \epsilon l \gg 1 \\
6^{-1/2}\epsilon^{-1/2}l^{1/2}, & \epsilon l \ll 1
\end{cases}
\tag{55}
$$

where the numerical factors are chosen for consistency with more precise results considered below (cf. eqn (56) and (57)).

For $\epsilon l \ll 1$ (moderate adsorption with $s_m \gg l$) both h and $\psi(r)$ can be obtained in a different way. First we note that $\psi(r)$ at $r \lesssim l$ is not affected by such small ϵ since self-similar structure in this region consists of short loops with $s \lesssim l$ for which the additional factor $\mathrm{e}^{-\epsilon s}$ is close to 1. Therefore $\psi(r)$ is given by eqn (43) for $r \lesssim l$. Furthermore, $\psi(r)$ for $r \gg l$ can be found using eqn (37) whose solution is given in eqn (38), hence h for $\epsilon l \ll 1$ is indeed defined by the second line in eqn (55). Using asymptotic behavior of K_0 in eqn (38) we get

$$
\begin{aligned}
\psi(r) &\sim \ln(h/r), \quad h \gg r \gg l; \\
\psi(r) &\sim \sqrt{h/r}\exp(-r/h), \quad r \gtrsim h
\end{aligned}
\tag{56}
$$

For stronger adsorption, $\epsilon l \gg 1$, the distal layer ($r \gtrsim l$) essentially disappears (it gets exponentially weak), while the proximal cylindrical layer becomes reduced due to suppression of aligned loops with length $s \gtrsim 1/\epsilon$. The resultant $\psi(r)$ in this regime is given by eqn (43) with the exponential cut-off factor established in ref. 6 and 7

$$
\psi(r) \sim (l/r)^{4/3}\exp\left(-(r/h)^{1/2}\right), \quad \Delta \lesssim r \lesssim h, \quad \epsilon l \gg 1
\tag{57}
$$

where h is defined by the first line in eqn (55), $h \ll l$. The argument of the exponent here comes from a balance between the elastic deformation energy of a half-loop and its desorption free energy $\epsilon Ts/2$ (cf. eqn (14)).[6,7]

The concentration profiles of polymer segments can be obtained based on eqn (38) and (57) using also eqn (25) and noting that at $r \ll l$ the orientational ($\underline{t}$) dependence of the function $\psi(\underline{r}, \underline{t})$ is concentrated within a small steric angle $\sim \Theta(r/l)^2 = (r/l)^{2/3}$ (and that the tail of orientational distribution of ψ at $\theta \gg \Theta(r/l)$ is unimportant for both $\psi(r)$ and $c(r)$). The result for $\epsilon l \ll 1$ is (cf. eqn (45)):

$$
c(r) \sim c_0 \cdot
\begin{cases}
(l/r)^{10/3}, & \Delta \ll r \ll l \\
[K_0(r/h)]^2, & h \gtrsim r \gtrsim l
\end{cases}
\tag{58}
$$

An alternative way to obtain the concentration profile $c(r)$ is presented in the Discussion point D3 (cf. eqn (80)). For $\epsilon l \gg 1$ it reads

$$
c(r) \sim c_0(l/r)^{10/3}\exp(-2(r/h)^{1/2}), \quad \Delta < r \lesssim h
\tag{59}
$$

In all the cases the distributions are suppressed beyond the cut-off length h, eqn (55).

It is of interest to obtain the fraction p of adsorbed segments (trains), which is equal to the probability that a segment of the

adsorbed chain is located at $r < \Delta$:

$$p \equiv p(\Delta, \infty) = \int_0^\Delta c(r) r \, dr \Big/ \int_0^\infty c(r) r \, dr \qquad (60)$$

(cf. eqn (36)). Using eqn (58) and (55) for $\epsilon l \ll 1$. we get

$$p \sim 1 \quad \text{for } \epsilon \gtrsim \epsilon_1;$$

$$p \sim \epsilon l \left[\left(\frac{l}{\Delta} \right)^{4/3} + \frac{\Delta^2}{l^2} \left(\ln \frac{1}{\epsilon \Delta} \right)^2 \right] \quad \text{for } \epsilon \lesssim \epsilon_1 \qquad (61)$$

where

$$\epsilon_1 \sim \frac{1}{l} \left(\frac{\Delta}{l} \right)^{4/3}, \quad \epsilon_1 l \ll 1 \qquad (62)$$

It remains to establish how the free energy ϵ (and h) depend on the adsorption strength u, $u > u^*$. The following relation coming from the theorem on small variations[50] is useful here (recall that $\tau \equiv 1 - u/u^*$, $\tau < 0$ here):

$$\frac{\partial F}{\partial \tau} = \left\langle \frac{\partial E}{\partial \tau} \right\rangle \qquad (63)$$

where $E = \int c(\underline{r}) U(r) d^2 r$ is the total energy of polymer/bar interactions for a given conformation (here $c(\underline{r})$ is normalized in such a way that $c(\underline{r}) d^2 r$ is the total length of chain segments inside the area element $d^2 r$), $\langle \cdot \rangle$ means conformational average (for equilibrium distribution), and $F \simeq -T\epsilon L$ is the adsorption free energy (cf. eqn (14)). Taking into account that $\partial E / \partial \tau = \int c(\underline{r}) [\partial U(r)/\partial \tau] d^2 r$,

$$\frac{\partial U(r)}{\partial \tau} \sim u^* T \text{ at } r < \Delta, \quad \partial U(r)/\partial t = 0 \text{ at } r > \Delta$$

and using eqn (63) we obtain (cf. ref. 6 and 7)

$$\frac{\partial \epsilon}{\partial \tau} \sim -u^* p \qquad (64)$$

where p is defined in eqn (60). Let us consider first the regime $\epsilon \lesssim \epsilon_1$. In this case eqn (64) and (61) lead to

$$\frac{\partial \epsilon}{\partial \tau} \simeq -C\epsilon \left(\frac{l}{\Delta} \right)^2 \left[1 + \left(\frac{\Delta}{l} \right)^{10/3} \ln^2 \left(\frac{1}{\epsilon \Delta} \right) \right] \qquad (65)$$

where C is a numerical constant depending on the shape of the attraction potential $U(r)$, cf. Fig. 3a (C is related to the numerical factors omitted in eqn (64) and (61)). It is important to remind here that all the above equations are valid for $\epsilon L \gtrsim 1$. If $\epsilon L \lesssim 1$, the system is nearly critical, hence, in particular, $c(r)$ is approximately given by eqn (45) with $h = R_{\text{coil}}$ (valid for $u = u^*$), leading (after integration in eqn (60)) to $p \sim (l/L)(l/\Delta)^{4/3} \equiv p_0$ in formal agreement with the second line in eqn (61) for $\epsilon \sim 1/L$. Thus

$$p \sim p_0 \quad \text{for } \epsilon \lesssim 1/L \qquad (66)$$

and p is defined by eqn (61) for larger ϵ. Then the second term in square brackets of eqn (65) is never important unless L is exponentially large which must not be the case (as discussed in point D2 of Section 4).

Using eqn (64) and (66) with 'initial' condition $\epsilon = 0$ at $\tau = 0$ we get $\epsilon \sim 1/L$ for $|\tau| \sim \tau_c$. Applying then the differential eqn (65) in the region $\tau < 0$, $|\tau| \gtrsim \tau_c$ we get

$$\epsilon \sim L^{-1} \exp(|\tau|/\tau_c), \quad \tau_1 > |\tau| > \tau_c \qquad (67)$$

where $\tau_c = \frac{1}{C}(\Delta/l)^2$ (cf. eqn (50)) and τ_1 is defined by the condition $\epsilon \sim \epsilon_1$ (cf. eqn (62)):

$$\tau_1 \simeq \tau_c \ln(\tau_c L/\lambda^*) \qquad (68)$$

For $\epsilon \gtrsim \epsilon_1$ (i.e. for $|\tau| \gtrsim \tau_1$) the polymer is mostly concentrated near the bar, so eqn (64) and (61) give $p \sim 1$ and

$$\epsilon \sim (\tau_c + |\tau| - \tau_1)/\lambda^*, \quad |\tau| > \tau_1 \qquad (69)$$

(recall that $1/\lambda^* \sim u^*$). Thus, the adsorbed chain partition function $\psi \propto e^{\epsilon L}$ (cf. eqn (13))§§ changes in the region $u > u^*$ ($\tau < 0$) as

$$\psi \sim \begin{cases} e^{\exp(|\tau|/\tau_c)}, & |\tau| < \tau_1 \\ e^{(L/\lambda^*)(\tau_c - \tau_1 + |\tau|)}, & |\tau| > \tau_1 \end{cases} \qquad (70)$$

Note double exponential increase of ψ at low $|\tau|$ and its further strong exponential increase beyond τ_1.

Now, using eqn (67), (69) and (55) we get the dependence of the terminal length, $h = h(\tau)$, for $\tau < 0$:

$$h \sim \begin{cases} \sqrt{Ll} \exp(-|\tau|/2\tau_c), & \tau_c \lesssim |\tau| < \tau_1 \\ l(\Delta/l)^{1/3}(\tau_c + |\tau| - \tau_1)^{-1/2}, & \tau_1 < |\tau| < \tau^* \\ \Delta/|\tau|^{3/2}, & 1 > |\tau| > \tau^* \\ \Delta, & |\tau| \gtrsim 1 \end{cases} \qquad (71)$$

where

$$\tau^* = (\Delta/l)^{2/3} \sim \lambda^*/l \qquad (72)$$

corresponds to the crossover, $\epsilon l \sim 1$ (cf. eqn (69)). Eqn (71) says that the cut-off length h is decreasing with $|\tau|$ (i.e. with u) above the critical point u^*. Exponential decrease of h from R_{coil} to $l(l/\Delta)^{2/3}$ is predicted for $\tau_c \lesssim |\tau| < \tau_1$, followed by power-law decreases from $l(l/\Delta)^{2/3}$ to l (for $\tau_1 < |\tau| < \tau^*$) and from l to Δ for $\tau^* < |\tau| < 1$. Therefore, the distal layer gets totally suppressed ($h \lesssim l$) at $|\tau| > \tau^*$. The concentration profile, $c(r)$, is defined in eqn (58) for $|\tau| < \tau^*$ and eqn (59) for $1 > |\tau| > \tau^*$.

The τ-dependence of the fraction p of trains can be found based on eqn (61), (66), (67) and (69):

$$p \sim \begin{cases} 1, & -\tau > \tau_1 \\ p_0 \exp(|\tau|/\tau_c), & 0 < -\tau < \tau_1 \\ (\lambda^* \tau_c/L)/(\tau + \tau_c)^2, & 0 < \tau < 1 \end{cases} \qquad (73)$$

where

$$p_0 = (l/L)(l/\Delta)^{4/3} \qquad (74)$$

§§ Note that this exponential factor, which is most important for $u > u^*$, equals 1 for $u \leq u^*$, so it was omitted in the previous sections.

To obtain the last line in the above equation we assumed (as before) that the chain is confined within the coil size from the bar and used the relation $p \sim \langle m \rangle \lambda^*/L$, where $\langle m \rangle$ is the mean number of train segments obtained in the next section (see eqn (101)) and λ^* is the mean train length (thus, $\langle m \rangle \lambda^*$ is the mean total length of all segments in contact with the bar).

4 Discussion

D1. Critical adsorption threshold u^*

In the previous sections we considered adsorption of an ideal stiff semiflexible macromolecule (WLC of diameter d_1) onto a straight bar (of diameter d_2) assuming that the Kuhn segment $l = l_1$ of the WLC is much larger than the range Δ of their attractive interactions, $l \gg \Delta$. Just for simplicity we also assumed that the repulsion range $d = d_1 + d_2$ is comparable with Δ.

Generally, to compensate for the hard-core repulsion from the bar (at $r < d \sim \Delta$) an attractive potential of magnitude $u_i \sim 1/\Delta$ may seems to be needed if the typical angle θ between the bar and the interacting polymer segment is $\theta \sim 1$ (cf. Fig. 3a).¶¶ However, the actual critical adsorption threshold u^* is much lower, $u^* \ll u_i$ (cf. eqn (31)) meaning that isotropic attraction (at $\theta \sim 1$) can be neglected. The reason is that at the critical point the hard-core repulsion is balanced by a strongly anisotropic attraction with typical $\theta \sim (\Delta/l)^{1/3} \ll 1$ (cf. eqn (19) with $r \sim \Delta$) leading to $u^* \sim \theta/\Delta \sim 1/\lambda^*$. It is due to such a balance between repulsion and attraction that both $\psi(\underline{r}, \underline{t})$ and $c(\underline{r}, \underline{t})$ become self-similar at the critical point in the proximal region $\Delta \ll r \ll l$.

D2. Athermal case of purely repulsive bar, $u = 0$

In Section 3.3 we found that at the adsorption threshold, $u = u^*$, the ψ-function (providing the chain-end distribution) follows the logarithmic law far from the bar, $r \gg l$. Let us consider the case of no attraction, $u = 0$. As long as we are interested in large distances, $r \gg l$, the WLC can be considered as 'flexible', that is, as a chain of $N = L/l \gg 1$ Kuhn segments with one end located at a distance $r \gtrsim l$ from the bar. Let us estimate the upper bound of the chain free energy increment, ΔF, due to repulsion interactions with the bar. Then ΔF is proportional to the mean number of contacts, n_c, between chain segments and the bar: $\Delta F \sim T n_c$ (by a contact we mean that an l-segment comes close to the bar within a distance $\sim \Delta$). Obviously,

$$n_c = \int_0^N p(n) \mathrm{d}n \qquad (75)$$

where $p(n)$ is the probability that the n-th segment (counted

¶¶ Such estimate of u_i is hinged on the second virial coefficient, B_2, for interaction of two (nearly) straight λ-segments of the WLC and the bar, $\Delta \lesssim \lambda \ll l$: B_2 should be negative for attraction to dominate. For a given angle θ a simple calculation gives (omitting numerical factors): $B_2 \sim \lambda^2 \sin\theta[d + \Delta(1 - e^{U/T})]$, where the first term in square brackets corresponds to the excluded volume, and the second term - to attraction between segments. Here $U \sim Tu\Delta/\sin\theta$ is the typical attraction energy. The condition $B_2 = 0$ for $\theta \sim 1$ and $\Delta \sim d$ then leads to $U \sim T$ and $u_i \sim 1/\Delta$.

from the fixed end) encounters a contact. Here $p(n)$ can be factorized as $p(n) \sim p_l(n)\Delta/l$, where $p_l(n)$ is the probability that the n-th l-segment gets within a distance $\sim l$ to the bar, and Δ/l is the conditional probability that in this case the minimal distance between the segment and the bar is $\sim \Delta$. By virtue of the Gaussian statistics of an ideal chain in 2 dimensions $p_l(n)$ is negligible if $nl^2 \ll r^2$, and for $nl^2 \gtrsim r^2$ (i.e. $n \gtrsim n_0 \sim r^2/l^2$) the probability $p_l(n) \sim 1/n$. Thus we get using eqn (75):

$$n_c \sim \int_{n_0}^N \frac{\Delta}{l} \frac{\mathrm{d}n}{n} \sim \frac{\Delta}{l} \ln\left(\frac{Nl^2}{r^2}\right) \qquad (76)$$

Recalling that the partition function $\psi = e^{-\Delta F/T}$, we get

$$\psi(r) \sim e^{-n_c} \sim \left(\frac{r^2}{Nl^2}\right)^{C\Delta/l} = \text{const } \exp(2C\ln(r/R_{\text{coil}})\Delta/l)$$

where C is numerical constant. Since $\Delta/l \ll 1$ and r is not exponentially large, the exponent above can be expanded leading to $\psi = \psi_0$,

$$\psi_0(r) \sim 1 + 2C(\Delta/l)\ln(r/R_{\text{coil}}), \quad l \ll r \lesssim R_{\text{coil}} \qquad (77)$$

Eqn (76) implies that $n_c \ll 1$, so that the partition function of a semiflexible loop is not really affected by interactions with the bar. In other words, long polymer loops around the bar show a nearly ideal statistics.

Note that the first term in the above equation corresponds to the partition function of a free chain with no interactions with the bar, $\psi_{\text{free}}(r) = 1$, while the second term reflects rare contacts with the bar. As $\Delta/l \ll 1$ is our main small parameter, the second term is small and can be neglected unless R_{coil} is exponentially large. The condition is: $\ln(R_{\text{coil}}/l) \ll l/\Delta$. To simplify the theory we choose to assume that the chain length is not exponentially large, i.e. that the above condition is satisfied. Hence $\psi = \psi_0(r) \simeq 1$ for $u = 0$ at $r \gg \Delta$.

D3. Fractal structure of weakly to moderately adsorbed chains

In Section 3.2 we considered the fractal distribution of loops in the proximal layer at the critical point, $u = u^*$. Below we show that a similar concept can be used to obtain the concentration profile in the distal region, and to study the statistics of trains.

Let us consider the system just slightly above the adsorption point ($u = u^*$) so that the reduced adsorption free energy ϵ is positive and small ($\epsilon l \ll 1$). In this case the proximal adsorbed structure (at $r \lesssim l$) is virtually the same as at the critical point: it involves trains close to the bar (at $r \lesssim \Delta$) and aligned loops (of length s, $\Delta \lesssim s \lesssim l$) with self-similar length distribution:

$$N_p(s) \propto s^{-4} \qquad (78)$$

where $N_p(s)$ is the number of aligned loops of length s (cf. eqn (34)). The distal region $r \gtrsim l$ involves longer loops with $s \gtrsim l$. Their length distribution $N_d(s)$ is also self-similar (for $l \ll s \ll 1/\epsilon$), but with a different exponent reflecting their flexible nature:

$$N_d(s) \propto s^{-1}e^{-\epsilon s} \qquad (79)$$

for $s \gg l$. Here $\epsilon s T$ is free energy penalty for desorption of a

loop of length s (see text above eqn (54)). The factor $1/s$ in eqn (79) reflects the probability that a 2D Gaussian chain of s units forms a loop.

Matching the two distributions at $s \sim l$, $N_p(l) \sim N_d(l)$, and applying the argument of Section 3.2 to obtain the polymer concentration profile $c(r)$ also in the distal region ($r \gtrsim l$) based on $N_p(s)$, $N_d(s)$ we get

$$c(r) \sim c_0\left(\frac{l}{r}\right)^{10/3}, \quad \Delta \lesssim r \ll l; \quad c(r) \sim c_0 \ln^2(h/r), \quad l \lesssim r \ll h \tag{80}$$

where $h \sim \sqrt{l/\epsilon}$ is the cut-off length (the terminal lateral size of the adsorbed chain), $h \gg l$. Note that eqn (80) are in agreement with eqn (58).

Both short and long loops must have both ends adjacent to train sections which serve as starting and end points for loops. Eqn (78) shows that most loops are short. The typical size of the shortest loops and trains is $s \sim \lambda^*$ (cf. eqn (30) and the text below eqn (32)). The trains connected by short aligned loops (of length $s < l$) can be combined together to get a supertrain whose ends are always adjacent with long loops (with $s > l$). On the other hand, each long loop is located between two supertrains along the chain contour. Thus, a supertrain is a continuous chain section oriented as a whole along the bar and located close to it (in the proximal layer).

Let us estimate the mean contour length, L_{st}, of one supertrain and their number, N_{st}. Obviously, the total number of long loops, N_{ll}, must be close to N_{st} (strictly, $N_{st} = N_{ll} + 1$). The terminal length of a long loop is $s_m \sim h^2/l \sim 1/\epsilon$. Furthermore, eqn (79) shows that

$$N_{ll} \sim \int_l^{s_m} N_d(s)\mathrm{d}s \tag{81}$$

Let $L(r_1, r_2)$ be the total polymer length in the region $r_1 < r < r_2$. Each long loop of length $s > 2l$ contributes a length $\sim l\ln(s/l)$ in the near-proximal region $l < r < 2l$ (the log-factor here comes from returns of internal l-segments of the loop into the near-proximal zone), hence

$$L(l, 2l) \sim \int_l^{s_m} l\ln(s/l)N_d(s)\mathrm{d}s \tag{82}$$

Using eqn (79), (81) and (82) we get

$$L(l, 2l) \sim l\ln(h/l)N_{ll} \tag{83}$$

As short loops (with $s \sim \Delta$) and trains dominate by mass in the proximal region, $L(0, \Delta)$ must be close to $N_{st}L_{st} \simeq N_{ll}L_{st}$: $L(0, \Delta) \sim N_{ll}L_{st}$. The above relations allow us to estimate L_{st}:

$$L_{st} \sim l\ln(h/l)L(0, \Delta)/L(l, 2l)$$
$$\sim l\ln(h/l)\int_0^\Delta c(r)r\,\mathrm{d}r \Big/ \int_l^{2l} c(r)r\,\mathrm{d}r \tag{84}$$

Using eqn (84) and (80) we then get the supertrain length:

$$L_{st} \sim l(l/\Delta)^{4/3}/\ln(h/l) \tag{85}$$

As follows from the scaling law, eqn (29), the masses of trains and supertrains are nearly the same (in particular, close to the

critical point), hence the supertrain mass fraction is $\sim p$ (see eqn (60) for the definition of p). At a very low ϵ ($\epsilon \ll \epsilon_1$ that is for $0 < u/u^* - 1 \lesssim \tau_1$) it is given by the second eqn (61):

$$p \sim \left(\frac{l}{\Delta}\right)^{4/3} l^2/h^2 \tag{86}$$

The number of supertrains therefore is

$$N_{st} \sim pL/L_{st} \sim \ln\left(\frac{h}{l}\right)\frac{Ll}{h^2} \tag{87}$$

This number $N_{st} \sim L\epsilon \ln\left(\frac{h}{l}\right)$ is nearly proportional to the total adsorption free energy $F_a = -TL\epsilon$, so that the free energy gain per supertrain is $\sim T$. By contrast, the potential (attraction) energy of a supertrain, E, is much larger by magnitude than its adsorption free energy F_a (near the critical point $u = u^*$): $E \sim -Tu^*L_{st} \sim -T(l/\Delta)^2$ (cf. eqn (31) and (85)), hence $|E| \gg T$. Therefore, the adsorption free energy F_a comes from a subtle balance of the adsorption energy E and confinement entropy of train sections and short loops.

Exactly at the critical point the cut-off length h is replaced by the chain size, R_{coil} (see text below eqn (39)): $h = R_{coil} = \sqrt{Ll}$ for $L \gg l$, hence (by virtue of eqn (86) and (87))

$$p \sim \left(\frac{l}{\Delta}\right)^{4/3} l/L, \quad N_{st} \sim \ln\left(\frac{L}{l}\right) \quad \text{at } u = u^*, \tag{88}$$

i.e. the critical adsorption involves just a few supertrains per chain. Note that the supertrain length $L_{st} \sim l(l/\Delta)^{4/3}$ (here we omitted the log-factor in eqn (85)) is much longer than the Kuhn segment l. Such a chain fragment would adopt an isotropic coil conformation in the free state. By contrast, a supertrain at the critical point is highly stretched along the bar: the ratio of its longitudinal size to lateral size is $L_{st}/l \sim (l/\Delta)^{4/3} \gg 1$.

The argument used above to obtain L_{st} can be applied also beyond the critical point, at $u > u^*$. It shows that eqn (85) stays valid also for $\tau < 0$, $|\tau| \lesssim \tau^* \sim (\Delta/l)^{2/3}$ corresponding to $\epsilon \lesssim 1/l$: the mean length of a supertrain in this case is

$$L_{st} \sim l(l/\Delta)^{4/3}/\ln(h/l), \quad 0 < -\tau \lesssim \tau^* \tag{89}$$

where $h = h(\tau)$ is defined in eqn (71). Thus L_{st} just slightly (logarithmically) grows as $|\tau|$ increases from 0 to τ^* reaching $L_{st} \sim 1/\epsilon_1 \sim l(l/\Delta)^{4/3}$ at $|\tau| \sim \tau^*$ where $\epsilon \sim 1/l$ (cf. eqn (69)). The number of supertrains $N_{st} = pL/L_{st}$ (cf. eqn (87)) changes with τ in a more complicated way: the fraction p of segments in the proximal ($r \lesssim l$) or contact ($r \lesssim \Delta$) layer is (cf. eqn (61) where the second term in square brackets can be neglected):

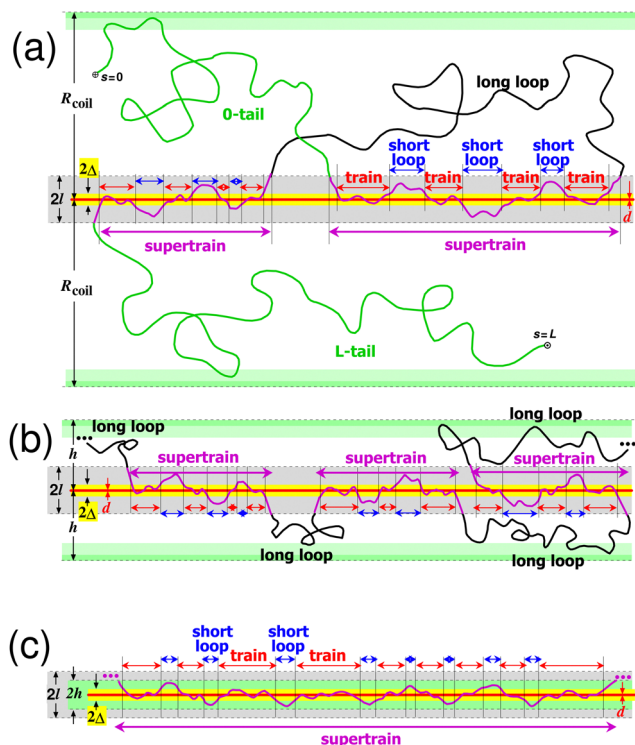$$p \sim (1 + \epsilon_1/\epsilon)^{-1} \tag{90}$$

where ϵ_1 is defined in eqn (62). Using the above equations (including eqn (89)) and $h^2 \sim l/\epsilon$ we get

$$N_{st} \sim \frac{L\epsilon_1}{1 + \epsilon_1 h^2/l}\ln(h/l), \quad \epsilon \lesssim 1/l$$

Recalling also the τ-dependence of h defined in eqn (71) we

Fig. 6 Fractal structure of semiflexible chain adsorbed onto a bar: (a) at the critical attraction point $u = u^\star$ ($\tau = 0$, $\epsilon = 0$); (b) above it, for moderate excess attraction strength $u = u^\star(1 - \tau)$, $\tau < 0$, $\tau_1 \lesssim |\tau| \lesssim \tau^\star = (\Delta/l)^{2/3}$, $\epsilon_1 \lesssim \epsilon \lesssim 1/l$; and (c) for strong attraction, $|\tau| \gg \tau^\star$, $\epsilon l \gg 1$. The main zones around the bar axis: steric repulsion zone of width $d = 2r_0$ (shown in red); attraction zone (yellow); proximal region involving short aligned loops, $r \lesssim l$ (grey); and distal zone extended to the terminal size h of the adsorbed chain, $l \lesssim r \lesssim h$ (within the light-green bars). Here $h \simeq R_{\mathrm{coil}} \sim \sqrt{Ll}$ for part (a), $l \lesssim h \lesssim R_{\mathrm{coil}}$ for (b) and $h \ll l$ for (c), cf. eqn (71). The chain can be viewed as an interlacing sequence of supertrains (shown as violet curve parts) and long loops of length $s \gtrsim l$ (black parts) between the two tails (shown in green only in (a)). Each supertrain is a sequence of trains (of length $s \sim \lambda^\star$ with $\theta \lesssim \theta^\star \sim (\Delta/l)^{1/3}$) connected with short aligned loops of length s, $\lambda^\star \lesssim s \lesssim l$. The trains and short loops are marked respectively with red and blue arrows.

finally obtain

$$N_{\mathrm{st}} \sim \begin{cases} \ln(L/l), & 0 < -\tau \lesssim \tau_{\mathrm{c}} \\ \exp(|\tau|/\tau_{\mathrm{c}}) \ln(h/l), & \tau_{\mathrm{c}} \lesssim -\tau < \tau_1 \\ (L/l)(\Delta/l)^{4/3}\ln(h/l), & \tau_1 < -\tau \lesssim \tau^\star \end{cases} \quad (91)$$

where $\tau_{\mathrm{c}} \sim (\Delta/l)^2$ and τ_1 is defined in eqn (68). Thus N_{st} exponentially increases from $N_{\mathrm{st}} \sim \ln(L/l)$ at $|\tau| \lesssim \tau_{\mathrm{c}}$ to the absolute maximum, $N_{\mathrm{st}} \sim (L/l)(\Delta/l)^{4/3} \ln(l/\Delta)$ at $|\tau| \sim \tau_1$, and then it slightly decreases down to $N_{\mathrm{st}} \sim (L/l)(\Delta/l)^{4/3}$ at $|\tau| \sim \tau^\star$.

The evolution of the trapped chain conformation as the attraction strength is increased (at $u \geq u^\star$) is illustrated in Fig. 6 for three characteristic regimes. At the critical point $u = u^\star$ (Fig. 6a) the large loops forming the distal region dominate by mass; the mean contour length of a large loop is $L_{\mathrm{ll}} \sim L/N_{\mathrm{ll}}$, where the number of large loops N_{ll} is close to the number of supertrains per chain, $N_{\mathrm{ll}} \simeq N_{\mathrm{st}} \sim \ln(L/l)$, which is just

logarithmic in L. The length of one supertrain is $L_{\mathrm{st}} \sim l(l/\Delta)^{4/3}/\ln(L/l)$, see eqn (85), and the total length of all adsorbed segments $L_\Delta = pL \simeq N_{\mathrm{st}}L_{\mathrm{st}} \sim l(l/\Delta)^{4/3} \ll L$, cf. eqn (85) and (88). Furthermore, the average number of trains in the chain is $\langle m \rangle \simeq L_\Delta/\lambda^\star \sim (l/\Delta)^2 \gg 1$ (cf. eqn (96)), hence each supertrain typically contains many ($m_{\mathrm{st}} \simeq \langle m \rangle/N_{\mathrm{st}} \gg 1$) trains. While the fraction of adsorbed segments $p \equiv p(\Delta,\infty) \sim (l/L)(l/\Delta)^{4/3} \ll 1$ (cf. eqn (88)) is extremely low, the fraction of adsorbed segments within each supertrain is $p(\Delta,l) \sim 1/2$, cf. eqn (35) and (36). In the case of moderate adsorption strength (see Fig. 6b), $\tau_1 \lesssim u/u^\star - 1 \lesssim \tau^\star$, where τ_1 is defined in eqn (68) and $\tau^\star = (\Delta/l)^{2/3}$, the cut-off distance h (for long loops) corresponds to the 2nd line of eqn (71), hence h decreases from $h \sim l(l/\Delta)^{2/3}$ at $u/u^\star - 1 \sim \tau_1$ to $h \sim l$ at $u/u^\star - 1 \sim \tau^\star$. The mean contour length of a long loop, L_{ll}, is $L_{\mathrm{ll}} \sim (h^2/l)/\ln(h/l)$; it decreases from $L_{\mathrm{ll}} \sim l(l/\Delta)^{4/3}/\ln(L/l)$ to $L_{\mathrm{ll}} \sim l$ at $u/u^\star - 1 \sim \tau^\star$. Noteworthily, the statistics of the chain for $s \lesssim l$ is practically not affected by the change $u^\star \to u = u^\star(1 + \tau^\star)$, see the text above eqn (78). In the regime of strong adsorption (see Fig. 6c), $u/u^\star - 1 \gg \tau^\star$ (where $\epsilon l \gg 1$, $h \ll l$) the number of supertrains shows an exponential decrease (while the mean supertrain length exponentially increases to keep $L_{\mathrm{st}}N_{\mathrm{st}} \simeq L$) rapidly reaching the minimal number $N_{\mathrm{st}} \simeq 1$ and the maximum length $L_{\mathrm{st}} \simeq L$. Note that for $0 < u/u^\star - 1 \lesssim 1$ both the typical train length and the typical length of a short loop (with $s \lesssim l$) are always comparable to $\lambda^\star$ (since it is the shortest loops of length $\sim \lambda^\star$ that dominate by number and by weight in accordance with eqn (34) and (35)).

D4. Chain-end partition function ψ for critical adsorption, $u = u^\star$

In the previous point D3 we harnessed the size distribution of loops to obtain the concentration profile $c(r)$ (eqn (80)). The partition function $\psi(r)$ at the critical point, $u = u^\star$, can be obtained is a similar way. It can be written as (cf. eqn (48) at $\tau = 0$)

$$\psi(r) = \psi_0(r) + \psi'(r) \quad (92)$$

where $\psi_0(r) \simeq 1$ is the statistical weight of non-adsorbed states with no trains (ψ_0 for $r \gg \Delta$ is also approximately equal to the statistical weight of conformations with no intersections at all between the chain and the interaction zone, $r < \Delta$, cf. eqn (77)), and $\psi'(r)$ is the statistical weight for conformations with at least one train.

Let us find $\psi'(r)$ at $u = u^\star$. Generally, the WLC conformations relevant for ψ' involve trains, loops and two tails (cf. Fig. 5). By definition, $\psi'(\underline{r})$ must be proportional to the probability density $\rho(\underline{r})$ that the end of the second tail (L-tail) is located at point $\underline{r}$. The function $\rho(\underline{r})$ can be deduced from the tail-length distribution $P(s)$ ($P(s)\mathrm{d}s$ is the probability that the tail length is between s and $s + \mathrm{d}s$). A tail does not significantly interact with the bar: the interaction energy per tail, E_{t}, is small, $|E_{\mathrm{t}}| \lesssim T$, since the return probability p_{r} that a given tail segment (of length $\lambda^\star$ located at the curvilinear distance $s' = \lambda^\star n'$ from the tail root, cf. Fig. 7) intersects the interaction zone, $r \lesssim \Delta$, is rapidly decaying with s': $p_{\mathrm{r}} \sim \Delta^2 \sqrt{n'}/r(s')^2 \sim (\lambda^\star/s')^{2.5} = (n')^{-2.5}$ (cf. eqn (3) and (33); note that the factor $\sqrt{n'}$ accounts for an increase
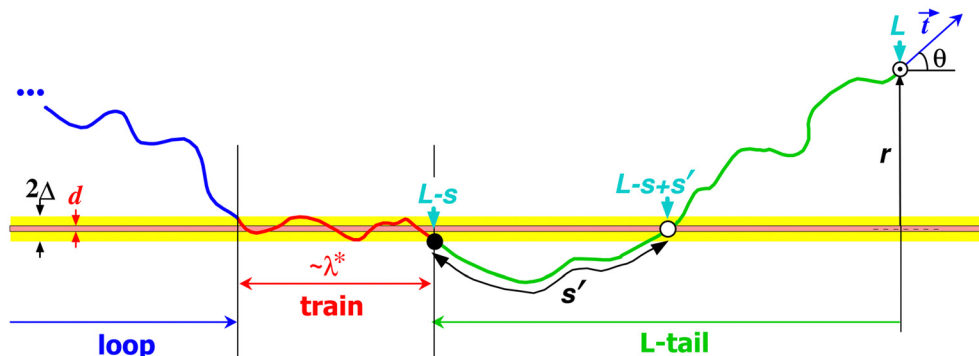
Fig. 7 A tail of length s and its inner point at the curvilinear distance $s' < s$ from its root (the last train and a part of the last loop are also shown). The curvilinear coordinates along the chain are marked in cyan: the tail root corresponds to $L - s$, its inner point to $L - s + s'$ and its free end to L.

of the typical intersection angle with n'). Summing p_r for all λ^*-segments with $n' > n$ we get $p_{rtot} = \sum_{n' > n} (n')^{-2.5} \sim n^{-1.5}$. Therefore, the total return probability p_{rtot} is small for large n, $p_{rtot} \ll 1$ for $n \gg 1$, hence a tail can be viewed as being virtually free (obeying the ideal statistics) leading to $P(s) = $ const at $\lambda^* \ll s \ll L$. More generally the tail statistical weight is proportional to $e^{-\epsilon s}$ which, however, equals 1 at the critical point where $\epsilon = 0$.

Taking into account that the typical lateral size of a tail, $r(s)$, is (*cf.* eqn (33))

$$r(s) \sim s^{3/2}l^{-1/2}, \quad \lambda^* \lesssim s \lesssim l; \quad r(s) \sim \sqrt{sl}, \quad s \gtrsim l \quad (93)$$

we find

$$\psi'(r) \propto \rho(r)$$
$$\propto l \int_{r(s) \gtrsim r} \frac{P(s)}{r(s)^2} ds \sim \begin{cases} \left(\dfrac{l}{r}\right)^{4/3} + \ln\dfrac{h}{l}, & \Delta \lesssim r \lesssim l \\ \ln\dfrac{h}{r}, & l \lesssim r \lesssim h \end{cases} \quad (94)$$

where $h \sim R_{coil} = \sqrt{Ll}$ and the condition $r(s) \gtrsim r$ accounts for the fact that short tails with $r(s) \ll r$ do not contribute to the statistical weight $\psi'(r)$ (more precisely, their contribution is negligible being exponentially small). The first term in the upper line in the r.h.s. of eqn (94) is due to short tails ($s \lesssim l$) which contribute to the proximal layer ($r \lesssim l$), and the second term comes from long tails ($s \gg l$) contributing everywhere (both proximal and distal layers). Eqn (94) is obviously in agreement with eqn (43) and (44). It shows that matching the asymptotics of $\psi'(r)$ at $r \ll l$ and $r \gg l$ assuming a crossover exactly at $r \sim l$ is not really accurate for the system we study: it is the long-tail contribution that always dominates $\psi'(r)$ at $r \sim l$, the contribution of short tails is weaker by a log-factor formally shifting the crossover to shorter r.

This effect is due to nearly ideal-chain statistics of loops and tails for WLC with $l \gg \Delta$ (see text above eqn (93)). The situation is different in the case of a flexible (Gaussian) chain adsorption onto a bar. The statistics of loops and tails is altered there due to excluded-volume interactions with the bar: a loop or a tail by definition must not enter the volume of the bar. As a result the statistical weights of both loops and tails decrease by log-

factors: $Z_{loop}(s) \propto \dfrac{1}{s(\ln s)^2}$, $Z_{tail}(s) \propto \dfrac{1}{\ln s}$ (these dependencies come from obvious convolution relations between statistical weights of ideal loops and tails with no interactions with the bar, and Z_{loop}, Z_{tail} with excluded volume of the bar). These log-factors for Gaussian chains compensate (in the eventual profiles $\psi(r)$, $c(r)$) for the analogous factors coming from the self-similar distributions of unperturbed loops and tails.

Note also that using eqn (25) and (94) and taking into account that the short-tail part of $\psi(\underline{r}, \underline{t})$ is concentrated within a steric angle $\sim \Theta(r/l)^2$ at $r \lesssim l$ (*cf.* eqn (19) and (41)) we come to the concentration profile $c(r)$ in agreement with eqn (45), (80) and (58). Here again we encounter the same effect: the contribution of long loops dominates $c(r)$ at $r \sim l$. Thus, generally, the correct way to establish the proper crossover between proximal ($r \ll l$) and distal ($r \gg l$) regimes for both $c(r)$ and $\psi(r)$ is to match the short-loop and long-loop branches of loop-length distribution at $s \sim l$.

D5. Trains and supertrains below the critical adsorption strength, $u \leq u^*$

Let us turn to the chain statistics at $u \leq u^*$. Generally we can classify the WLC states near the bar according to the number m of train segments, $m = L_{tt}/\lambda^*$, where L_{tt} is the total length of all trains and λ^* is the average length of a train segment (whose typical energy of interaction with the bar is $\sim T$ at $u \sim u^*$). The mean L_{tt} (at a given u) is equal to $\langle L_{tt} \rangle = pL$ (*cf.* eqn (60)). At $u = u^*$ it is equal to

$$L_{tt} = pL \sim \left(\frac{l}{\Delta}\right)^{4/3} l \quad (95)$$

(*cf.* eqn (88)) corresponding to the mean number of train segments (of length $\sim \lambda^*$, *cf.* eqn (30))

$$m_0 \equiv \langle m \rangle = pL/\lambda^* \sim (l/\Delta)^2 \quad (96)$$

Therefore m_0 is large, but, on the other hand, it is much smaller than the maximum number of such segments in the chain, $m_0 \ll L/\lambda^*$ (here we consider adsorption of a sufficiently long chain, $L \gg L_{tt}$).

Let us find the probability distribution of m first at $u = u^*$, namely, the probability $p_0(m)$ for the chain to have exactly $m \geq 1$ train segments. Below we argue that this distribution is exponential. Indeed, it is clear that if a λ^*-segment ending at point $L - s$ is adsorbed, one of the next segments (along the chain) would be also adsorbed with high probability, so that the probability q that no further segment is adsorbed is small, $q \ll 1$. Moreover, to demand that there are no trains beyond the point $L - s$ is equivalent to saying that the segment $(L - s, L)$ is a tail (cf. Fig. 7). The tail probability is independent of its length s (provided that $s \gg \lambda^*$; cf. point D4), which means that q is constant: it does not depend on s. Moreover, q is obviously independent of whatever is the chain conformation prior to the point $L - s$. Therefore, the process is Markovian and $p_0(m) \propto (1 - q)^m$ leading to

$$p_0(m) \simeq (1/m_0)\exp(-m/m_0) \tag{97}$$

The partition function $\psi(r)$ can be therefore written as

$$\psi(r) \simeq 1 + \sum_{m \geq 1} \psi'(r)p_0(m) \tag{98}$$

where the term '1' stands for $\psi_0(r) \simeq 1$, the partition function with no trains (cf. text below eqn (49)), and $\psi'(r) \simeq \psi_1(r) - 1$, cf. eqn (49), is the partition function reflecting all conformations involving adsorbed segments (trains).‖

The chain potential energy in the state m is $E_m = -Tum\lambda^*$ (omitting a numerical prefactor). At $\tau > 0$ the Boltzmann weights, W_m, of m-states ($W_m = e^{-E_m/T} = e^{um\lambda^*} = e^{(1-\tau)m}$ since $u^*\lambda^* = 1$, see eqn (30) and (31)) change due to the additional factor $e^{-\tau m}$ destabilizing the states with longer trains and leading to a lower total statistical weight

$$\psi(r) \simeq 1 + \sum_{m \geq 1} \psi'(r)p_0(m)e^{-\tau m} = 1 + \psi'(r)/(1 + \tau m_0) \tag{99}$$

The last equation is equivalent to eqn (48) where k should be identified with m_0 defined in eqn (96). Eqn (48) is justified this way.

The probability to have exactly $m \geq 1$ train segments is

$$p(m|r) = \psi'(r)p_0(m)e^{-\tau m}/\psi(r)$$

where the numerator in the r.h.s. is the statistical weight of the m-state (cf. eqn (99)). As the chain is delocalized at $\tau > 0$ (i.e. its segments are mostly located far from the bar, at $r \sim R_{coil}$), averaging of $p(m|r)$ over r (to get the averaged distribution $p(m)$) is equivalent to setting $r \sim R_{coil}$. Eqn (49) and (41) then give $\psi'(r) \sim \psi(r) \sim 1$, so

$$p(m) \sim p_0(m)e^{-\tau m}, \quad m \geq 1 \tag{100}$$

Hence (cf. eqn (97))

$$\langle m \rangle = \sum_m mp(m) \sim m_0/(1 + \tau m_0)^2 \tag{101}$$

Thus $\langle m \rangle$ decreases from $\langle m \rangle \sim m_0$ at $\tau \lesssim (\Delta/l)^2$ to $\langle m \rangle \sim 1$ at $\tau \sim \Delta/l$ and to $\langle m \rangle \sim 1/m_0$ at $\tau \sim 1$. The latter result means that

‖ Note that $\psi'(r)$ is related to the tail-length distribution (see point D4) which is independent of m since $m\lambda^* \ll L$ (cf. text below eqn (96)).

at $\tau \sim 1$ just a single train segment (of length $\sim \lambda^*$) is formed with low probability $p_1 \sim (\Delta/l)^2$. This probability can be obtained independently and more directly as

$$p_1 \sim N_t p_t \tag{102}$$

where $N_t \sim L/\lambda^*$ is the number of λ^*-segments in the chain, and p_t is probability that a chosen segment is in the train state, so that it is located within distance Δ from the bar and oriented parallel to it (within the deviation angle θ^*): $p_t \sim (\Delta^2/R_{coil}^2)(\theta^*)^2 \sim \Delta^2(\theta^*)^2/(Ll)$. Using eqn (102), (30) and (32) we then get again $p_1 \sim (\Delta/l)^2$.

Note that in eqn (101) the averaging is done over all conformations including those with no train at all. By contrast, the mean number of train segments, $\bar{m}$, averaged over only those conformations that involve a train is

$$\bar{m} = \sum_{m \geq 1} mp(m) \Big/ \sum_{m \geq 1} p(m) \simeq \frac{m_0}{1 + \tau m_0} \tag{103}$$

Thus $\langle m \rangle \sim \bar{m} \sim m_0$ at $\tau = 0$.

More generally, eqn (101) and (103) mean that a few super-trains of $\sim \bar{m}$ λ^*-segments are formed with probability $p_{st} \simeq \sum_{m \geq 1} p(m) = \langle m \rangle/\bar{m}$. (Note that the number N_{st} of super-trains is just logarithmic at $u = u^*$, cf. eqn (88); this number is even lower at $u < u^*$ since formation of yet another supertrain must be obviously less probable with a weaker attraction. This argument backs the idea of zero or a few supertrains per chain.) Thus, if a supertrain is formed (which is equivalent to demanding that $m \geq 1$), its mean length is:

$$L_{st}(\tau) \sim \lambda^*\bar{m} \sim l(l/\Delta)^{4/3}/(1 + \tau/\tau_c), \quad 1 \geq \tau \geq 0 \tag{104}$$

and the probability to have at least one supertrain is

$$p_{st}(\tau) \sim 1/(1 + \tau/\tau_c) \tag{105}$$

For $\tau = 0$ the above equations give $p_{st}(0) \sim 1$ and $L_{st}(0) \sim l(l/\Delta)^{4/3}$ in agreement with eqn (85) (recall that the log-factor is neglected in eqn (104)), while for $\tau = 1$ we get $L_{st}(1) \sim \lambda^*$, $p_{st}(1) \sim (\Delta/l)^2$.

Note that the mean potential energy is $E = \langle E_m \rangle \sim -T \langle m \rangle (1 - \tau) \sim -T(1 - \tau)m_0/(1 + \tau m_0)^2$. This energy is large, $|E| \gg T$, for $\tau \ll \Delta/l$, i.e. close to the critical point.

D6. Two WLCs instead of WLC + straight 'bar'

Having considered WLC adsorption on a bar, let us return to the original problem of two WLCs (A and B chains of length $L \gg l$) with local attractive interactions (cf. Fig. 1 and 2). As before here and below (to the end of Discussion section) we assume that attraction is effective only between segments of different chains. As stated in Section 2.1 this problem is equivalent to one WLC with effective Kuhn segment l^* near a bar as long as we are interested in distances $r \ll l^*$. In the general case of two chains with different Kuhn segments, l_1 and l_2, the length l^* is defined by the relation

$$1/l^* = 1/l_1 + 1/l_2 \tag{106}$$

The condition $r \ll l \equiv l^*$ points to the adsorption regime, $u > u^*$, $\epsilon l \gg 1$ which corresponds to $\tau < 0$, $|\tau| \gg \tau^*$ (cf. eqn (72)).
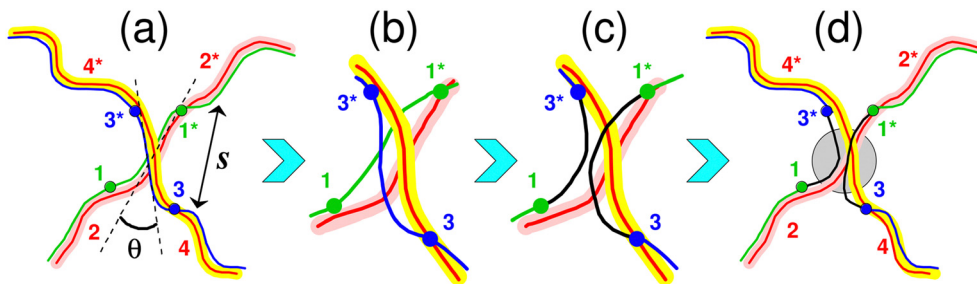
Fig. 8 Branching by strand exchange between two paired complementary chains (*cf.* Fig. 1): 1 + 2 and 3 + 4 pairs virtually intersect each other. The red strands (2 and 4) stay intact during exchange; their attractive zones (for the other two chains) are shown in pink and yellow. The exchange involves fragments (11*) and (33*) of length s making a small angle $\theta \sim (s/l)^{1/2}$ with each other. The strands 1 and 3 break and recombine in a different way during the exchange: the initial fragments (11*) and (33*) in (a) and (b) are converted into (13*) and (31*) in (c) and (d). The new branching point is marked with grey circle.

In this case the chains should form a double-chain complex wherein the chain trajectories are nearly parallel to each other and their lateral separation r is limited by h, $r \lesssim h$, where $h \sim \Delta/|\tau|^{3/2} \ll l$ (*cf.* the 3rd line of eqn (71)). Moreover, for $|\tau| \gg \tau^*$ the typical distance r is even shorter, $r \lesssim \Delta$, while the mass fraction of 'loops' of larger lateral size ($r \gg \Delta$) is small. Short loops (of length $s \ll \lambda^*/|\tau|$) must show the self-similar size distribution (in the range $\Delta \ll r \ll h$): the mass fraction of loops with lateral size $\sim r$ is

$$p(r) \propto r^{-4/3} \qquad (107)$$

(*cf.* eqn (29), (45) and (59) and note that $p(r) \propto r^2 c(r)$). Hence it is the shortest loops of length $\sim \lambda^*$ with $r \sim \Delta$ that dominate by mass.

Generally, the double-chain complex is stable if $L\epsilon \gg 1$, where ϵ is defined in eqn (67) and (69). In particular, the stability criterion for $-\tau \sim \tau^* = (\Delta/l)^{2/3}$ is $L \gg l$.

D7. Branching of double chains and gelation at $-\tau \gg \tau^*$

Let us consider formation of double-chain complex in the regime of strong attraction, $\epsilon l \gg 1$, when the distal layer is suppressed (*cf.* Section 3.5) and almost all polymer fragments are involved in the supertrain structure whose total length tends to L. Only short 'proximal' loops (with $s \ll l$) are allowed within this mostly double-chain structure (*cf.* Fig. 1a). Their length distribution is defined in eqn (78). The number of loops with length $\sim s$ is $N_{\text{loop}}(s) \propto s N_{\text{p}}(s)$, so

$$N_{\text{loop}}(s) \sim N_{\text{loop}}(\lambda^*)(\lambda^*/s)^3, \quad s \lesssim l \qquad (108)$$

where $N_{\text{loop}}(\lambda^*) \sim L/\lambda^*$ is the reference number of the shortest loops of size $s \sim \lambda^*$.

If two double-chain fragments pass close by, they can form a branching point by chain exchange[29] as shown in Fig. 8. An exchange occurs when 2 short loops (11) and (33) transform into 2 transmuted loops (13) and (31) (*cf.* Fig. 8b). For loops of length $\sim s$ the exchange probability is significant if both loops are aligned similarly (within the angle $\theta \sim \theta(s) \sim (s/l)^{1/2}$) and overlap in space (occupy the same volume $v_{\text{ov}} \sim s r(s)^2$, where $r(s)$ is defined in eqn (33)). The above conditions imply that the two double chains involved in the exchange must intersect at a

small angle $\sim \theta(s)$. The probability of exchange for two arbitrarily chosen s-loops is therefore

$$p_{\text{ex}} \sim v_{\text{ov}}\theta^2/V \qquad (109)$$

where V is the total volume occupied by the double-chain. Eqn (108) and (109) lead to the following number, $N_{\text{ex}}(s)$, of exchange bridges of length $\sim s$:

$$N_{\text{ex}}(s) \sim p_{\text{ex}} N_{\text{loop}}(s)^2 \sim \frac{L^2}{V} \frac{\lambda^{*4}}{l^2 s} \qquad (110)$$

Clearly, it is the shortest 'bridging' loops of $s \sim \lambda^*$ that dominate by number, $N_{\text{ex}} \sim N_{\text{ex}}(\lambda^*)$:

$$N_{\text{ex}} \sim n_1(\Delta/l)^2 \qquad (111)$$

where

$$n_1 = L^2 l/V \qquad (112)$$

is the typical number of overlapping l-segments in the double chain. Each exchange (branching) point brings about the factor ~ 2 in the partition function of the system (thus decreasing the total free energy by $\sim T$), so the total exchange free energy is

$$F_{\text{ex}} = -T \ln Z_{\text{ex}} \sim -T N_{\text{ex}} \sim -T n_1(\Delta/l)^2 \qquad (113)$$

The free energy F_{ex} due to exchange branching is equivalent to a weak effective attraction of polymer segments (within the second virial approximation) which, just like formation of reversible bonds in solutions of associative polymers,[51] can cause phase separation. The excluded-volume repulsion of double-chain segments results in analogous positive free energy contribution

$$F_{\text{rep}} \sim T n_1(\Delta/l) \qquad (114)$$

where Δ/l stands for B/l^3, $B \sim l^2 \Delta$ being the second virial coefficient for steric interaction of 2 segments of length l.*** Obviously F_{rep} dominates over F_{ex}, so the double chain remains in the expanded (coil) state for $\epsilon l \gtrsim 1$ (that is, for $-\tau \gtrsim \tau^*$). For $l \ll L \lesssim (l/\Delta)^2 l = L_{\text{m}}$ (*i.e.* in the regime of a Gaussian coil which

---

*** Recall that we consider a long double-chain, $L \gg l$, where double-chain fragments pass by each other at arbitrary angles.
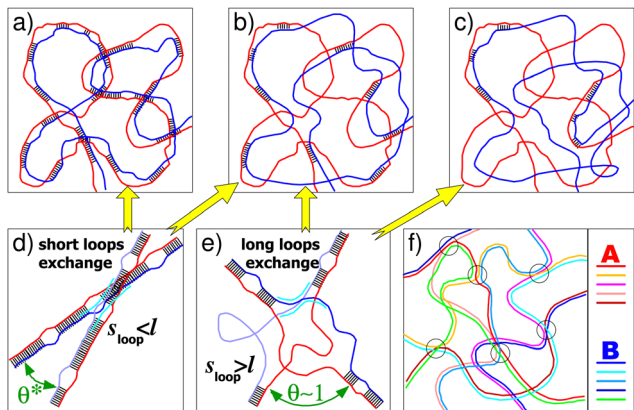
Fig. 9 Internal structure of a complex of two complementary semiflexible chains, A (red) and B (blue), for various mutual attractions u, $-\tau \equiv u/u^{*} - 1$: (a) strong attraction ($-\tau \gtrsim \tau^{*} \equiv (\Delta/l)^{2/3}$, cf. sect. D7), (b) moderate attraction ($\tau_c^{*} \lesssim -\tau \ll \tau^{*}$, $\tau_c^{*} \equiv (\Delta/l)^{14/9}$, cf. sect. D8), and (c) weak attraction ($\tau > 0$, cf. sect. D9). In (d) and (e) two distinct modes of branching are shown: by exchange between short loops dominating for $-\tau \gg \tau_{\text{loops}} \equiv (\Delta/l)^{14/15}$ (d), and by chain exchange involving long loops valid for $-\tau \lesssim \tau_{\text{loops}}$ (e), cf. eqn (131). For $|\tau| \lesssim (\Delta/l)^{4/3}$ the exchange of long loops leads to collapse of the complex (cf. eqn (132) and (141)). Part (f) shows a gel formed at polymer volume fraction $\phi > \phi_{\text{g}} \sim l/L$ for strong attraction ($-\tau \gtrsim \tau^{*}$), cf. eqn (116). The branching points are indicated with circles. All A-chains are equivalent, as well as all B-chains, different shades of red and blue are used for clarity.

is not really swollen by repulsive steric interactions) the coil volume $V \sim R_{\text{coil}}{}^3 = (Ll)^{3/2}$, so we find

$$N_{\text{ex}} \sim (L/l)^{1/2}(\Delta/l)^2 \ll 1 \quad (115)$$

The exchange branching therefore can be neglected in this regime (see Fig. 9a).

However, the situation may be different in the case of a semidilute solution of WLCs, $c > c^{*}$, where c is the number of Kuhn segments per volume, and $c^{*} \sim N/R_{\text{coil}}{}^3 \sim L^{-1/2}l^{-5/2}$ is the coil overlap concentration ($N = L/l$, $R_{\text{coil}} = \sqrt{Ll}$). In this case the total number of Kuhn segments is cV, so the mean number of overlapping l-segments is $n_l \sim (cV)^2 l^3/V = c^2Vl^3$, hence, by virtue of eqn (111), $N_{\text{ex}} \sim c^2Vl\Delta^2$, and the number of junctions per double-chain is $\nu = N_{\text{ex}}L/(cVl) \sim cL\Delta^2$. A gel (cf. Fig. 9f) is formed in the solution if $\nu > 1$ (as follows from the Flory theory[52] in the case of high functionality corresponding to a large number of short loops per chain in the present case) leading to the gelation criterion

$$c > c_{\text{g}} \sim 1/(L\Delta^2) \quad (116)$$

Note that the ratio $c_{\text{g}}/c^{*} \sim l^{5/2}\Delta^{-2}L^{-1/2} \gg 1$ is large (if $L \lesssim L_{\text{m}}$) and that the polymer volume fraction at the gelation point, $\phi_{\text{g}} \sim c_{\text{g}}\Delta^2 l \sim l/L$, is small since $L \gg l$ (semiflexible polymers). Moreover, taking into account that nematic transition in WLC solutions takes place at[53]

$$\phi_{\text{in}} \sim 10\Delta/l \quad (117)$$

we conclude that the gelation is predicted in the isotropic state if $L \gtrsim l^2/(10\Delta)$, while at shorter L it should occur in the nematic regime, $\phi > \phi_{\text{in}}$.

D8. Globule formation at $-\tau \ll \tau^{*}$

Let us turn to the regime of weaker attraction, where $\epsilon l \ll 1$ and the terminal separation h between interacting chains exceeds the Kuhn segment, $h \gg l$. Here the double-chain structure is less perfect: it involves defects like large loops of size $\gg l$ (Fig. 9b) with two strands (subloops) of length $s_1 \gg l$ and $s_2 \gg l$ (cf. Fig. 10a). The partition function of such a loop, $Z_{\text{loop}} \propto (s_1 + s_2)^{-3/2}$, reflects its 3-dimensional and flexible nature. Integrating Z_{loop} over s_1 and s_2 with $s_1 + s_2 \sim s$ we get the number of loops of length $\sim s$,

$$N_{\text{ll}}(s) \sim Z_{\text{loop}}s^2 \propto s^{1/2}, \quad s_{\text{m}} \gtrsim s \gtrsim l \quad (118)$$
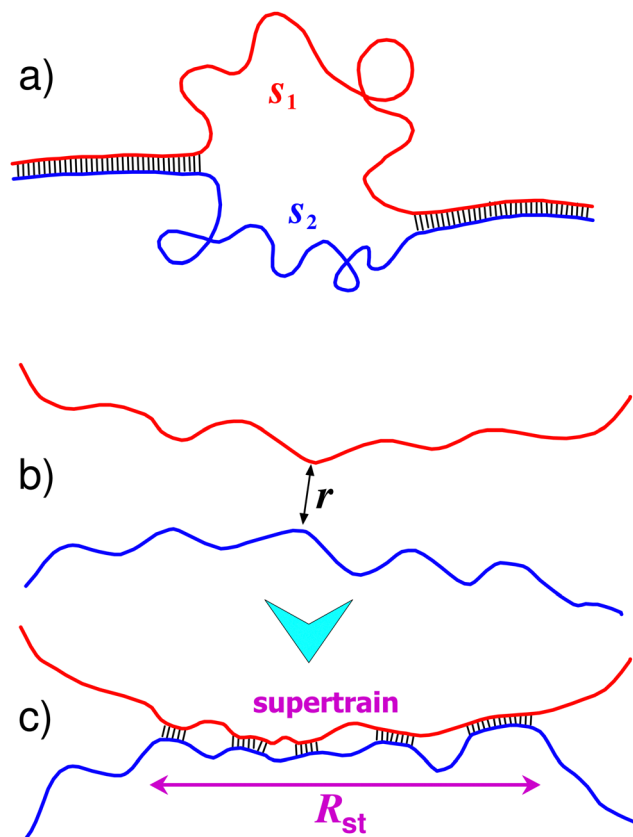
Here

$$s_{\text{m}} \sim 1/\varepsilon \quad (119)$$

is the terminal loop length (see Section 3.5). Matching eqn (108) and (118) at $s \sim l$ we get

$$N_{\text{ll}}(s) \sim \frac{L\lambda^{*2}}{l^3}(s/l)^{1/2}, \quad s_{\text{m}} \gtrsim s \gtrsim l \quad (120)$$

for a double-chain of length L. The length fraction of all long loops is

$$\varphi \sim \frac{1}{L}\int_l^{s_{\text{m}}} sN_{\text{ll}}(s)\mathrm{d}s/s \sim \lambda^{*2}s_{\text{m}}^{3/2}l^{-7/2} \quad (121)$$

Fig. 10 (a) A double chain with a 'molten' fragment involving two subloops, s_1 and s_2. (b) Two complementary chains passing by each other at a minimal distance $r \sim l$. (c) An alternative paired state of the chains involving a supertrain of size R_{st}.

Let us assume for simplicity that the tightly paired double-chain fragments (with separation $r \ll l$) dominate by mass, so that $\varphi \lesssim 0.5$. On using eqn (121) and (119) this condition leads to

$$s_m \lesssim l(l/\Delta)^{8/9}, \quad \epsilon l \gtrsim (\Delta/l)^{8/9} \quad (122)$$

On the other hand, using also eqn (64) with $p \simeq 1 - \varphi \sim 1$ (where p is the fraction of paired segments) and noting that $\epsilon = 0$ at $\tau = 0$ we get by integration

$$\epsilon l \sim -\tau/\tau^* \quad (123)$$

(cf. eqn (72)), so that the regime we study, $(\Delta/l)^{8/9} \lesssim \epsilon l \ll 1$, corresponds to

$$\tau_c^* \lesssim -\tau \ll \tau^* \quad (124)$$

where

$$\tau_c^* = (\Delta/l)^{14/9} \quad (125)$$

Eqn (123) ensures that $s_m \sim 1/\epsilon$ is large: $s_m \sim l\tau^*/|\tau| \gg l$. From eqn (120) it is clear that the total number of large loops N_{ll} is dominated by the largest loops of length $s \sim s_m$ whose number is

$$N_{ll} \sim L(\lambda^*)^2 l^{-3}(\tau^*/|\tau|)^{1/2} \quad (126)$$

The above equation ensures that $N_{ll} \gg 1$ if $L \gg l(l/\Delta)^{4/3}$. The latter condition essentially says that the chain length L must be much larger than the typical supertrain length (cf. eqn (85)); it was already adopted in point D5 (see text below eqn (96)).

Long flexible loops (of length $s \sim s_m$) provide an additional channel for crosslinking (branching) of double chain fragments (Fig. 9e). The dominant contribution to the number of junctions (exchange points) due to long loops, $N_{ex(ll)}$, comes from exchanges between overlapping loops (cf. eqn (110)):

$$N_{ex(ll)} \sim N_{ll}^2 \nu_{ll}/V \quad (127)$$

where

$$\nu_{ll} \sim (s_m l)^{3/2} \quad (128)$$

is the effective (accessible) volume occupied by a long loop, and ν_{ll}/V is the overlap probability for any pair of such loops. Using the above two equations and eqn (126) we get

$$N_{ex(ll)} \sim n_l(\tau^*/|\tau|)^{5/2}(\Delta/l)^{8/3} \quad (129)$$

where n_l is defined in eqn (112). Summing the contributions of short and long loops (cf. eqn (111) and (129)) we get the total number of junctions

$$N_{ex(tot)} \sim n_l\left(\frac{\Delta}{l}\right)^2\left(1 + \tau^{*7/2}/|\tau|^{5/2}\right), \quad F_{ex} \sim -TN_{ex(tot)} \quad (130)$$

Obviously, long loops become more important if (recall that $\tau^* = (\Delta/l)^{2/3}$)

$$-\tau \lesssim (\Delta/l)^{14/15} \equiv \tau_{loops} \ll \tau^* \quad (131)$$

(cf. Fig. 9e). Comparing the exchange free energy F_{ex} (cf. eqn (130)) with the repulsion energy, eqn (114), we find that exchange attraction dominates if

$$-\tau \lesssim (\Delta/l)^{4/3} \equiv \tau_g \quad (132)$$

In the regime of eqn (132) the total second virial coefficient becomes negative leading to collapse and gelation of the double-chain polymer coil, that is, to formation of a crosslinked globular complex. The junctions are mostly due to long loops in this regime (cf. eqn (132) and (131)). The collapse stops once all long loops become paired, the corresponding condition is $N_{ex(ll)} \sim N_{ll}$ leading to $V \sim \nu_{ll}N_{ll}$ (note that $N_{ll} \gtrsim L\Delta/l^2 \gg 1$ at $-\tau \lesssim \tau_g$, cf. eqn (126), and $\nu_{ll} \sim l^3(\tau^*/|\tau|)^{3/2}$, cf. eqn (128)). The concentration of the globular complex (and the corresponding volume fraction) therefore are

$$c \sim L/(lV) \sim l^{-3}(|\tau|/\tau_g)^2, \quad \phi \sim c\Delta^2 l \sim (\Delta/l)^2(|\tau|/\tau_g)^2 \quad (133)$$

Obviously c is independent of the total chain length L and $c \lesssim l^{-3}$ in the regime of eqn (132). Hence polymer volume fraction $\phi \lesssim (\Delta/l)^2$ is low, $\phi \ll \phi_{in}$ (cf. eqn (117)), so the globule is predicted to remain isotropic.

Interestingly and somewhat paradoxically, the collapse is predicted here as attraction of polymer chains gets weaker. The reason is that for strong attraction a double-strand (ladder) structure is most favorable (note that we assume a strictly monodisperse system). The double chain complexes do not aggregate further as all attractive interactions (bonds) are already saturated in the paired state (cf. Fig. 1c).

D9. Bridging by double-chain fragments and collapse near and below u^*

Let us first consider a pair of long WLCs at the critical point, $u = u^*$, in a volume V. We assume that $V \lesssim V_{coil} = R_{coil}^3 = (Ll)^{3/2}$. In the case of WLC adsorption on a straight bar we have shown (see point D3) that the typical length of paired (supertrain) fragments is

$$L_{st} \sim l(l/\Delta)^{4/3} \gg l \quad (134)$$

(see eqn (85) where we omit the log-factor). It is reasonable to assume (as verified below) that for $L \gg L_{st}$ the mass fraction of paired fragments is small (see Fig. 9c). The pairing occurs readily once two l-segments (belonging to different chains) come to each other closer than their size, $r \sim l$ (cf. Fig. 10b). Indeed, as follows from eqn (41) (last line), in this case the statistical weight of a paired state (supertrain in Fig. 10c), $\psi' \simeq \psi_1 - \psi_0 \sim \ln(R_{coil}/l)$, gets larger than the statistical weight ψ_0 of the state with no contacts between the chains, $\psi_0 \simeq 1$. Such ψ' leads to double-strand (supertrain) formation with probability $p = \psi'/(\psi_0 + \psi') \gtrsim 1/2$.

Let us find the total number of double-strand bridges. To this end it is useful to consider a WLC as a sequence of $N = L/L_{st}$ supertrain fragments and to find the number n of such over-lapping fragments:

$$n \sim N^2 R_{st}^3/V \quad (135)$$

where $R_{st} \sim (lL_{st})^{1/2}$ is the supertrain size (by virtue of Gaussian statistics of chain fragments at length-scales $\gtrsim l$). Obviously each pair of overlapping L_{st}-fragments must give rise to

formation (with high probability p) of a double-strand fragment (of length $\sim L_{st}$) bridging the WLCs. The number of bridges is therefore $n_{br} \sim n$, and the corresponding free energy is (in analogy with eqn (113))

$$F_{br} \sim -Tn_{br} \qquad (136)$$

The mass fraction of paired fragments is $\phi_{pf} \sim L_{st}n_{br}/L$. For $V \sim R_{coil}^3$ and $n_{br} \sim n$ we thus get (using eqn (135))

$$\phi_{pf} \sim (L_{st}/L)^{1/2}$$

meaning that $\phi_{pf} \ll 1$ for $L \gg L_{st}$ as stated above.

Using eqn (134) and (135) we get

$$n_{br} \sim n \sim n_l(\Delta/l)^{2/3} \qquad (137)$$

where n_l is defined in eqn (112). Comparing eqn (136) and (137) with eqn (114) for the free energy F_{rep} due to steric repulsion we find that bridging attraction always wins ($|F_{br}| \gg F_{rep}$) leading to a collapse of the bridged WLCs, that is, formation of a globule with finite density (volume fraction $\phi = L\Delta^2/V$). The equilibrium ϕ can be estimated using the condition that the maximum number of bridges is attained, *i.e.* that the bridged double-chain fragments occupy most of the chain, $n_{br} \sim N$, leading to

$$\phi \sim (\Delta/l)^{8/3} \qquad (138)$$

Note that the globule remains isotropic since the nematic transition occurs at a much larger concentration, $\phi_{in} \sim 10\Delta/l$.[53] For a binary solution of semiflexible polymers with stoichiometric 1:1 composition and with attraction only between segments of different kind (A and B), eqn (138) also defines the density of polymer precipitate at $u = u^\star$ ($\tau = 0$).

The obtained results remain valid also slightly below $u^\star$, at $0 < \tau \lesssim \tau_c \sim (\Delta/l)^2$ (*cf.* eqn (50)) where the supertrain length remains nearly the same (*cf.* eqn (104)). Moreover, the approach outlined above can be applied also at $\tau \gtrsim \tau_c$. As τ increases above τ_c the bridging gets weaker. At $\tau \gg \tau_c$ the statistical weight for supertrain formation (in the case of a mild overlap of two mutually attracting l-segments, $r \sim l$) decreases from $\psi' \simeq \psi - 1 \sim 1$ to $\psi - 1 = \psi_{br} \sim \tau_c/\tau$ (we neglect log-factors here; *cf.* eqn (51) and (99)). The typical supertrain length decreases in parallel (*cf.* point D5 of Section 4, eqn (104)),

$$L_{st}(\tau) = L_{st}\tau_c/\tau \qquad (139)$$

where L_{st} is defined in eqn (134).

The argument used above to estimate the number of bridges remains valid provided that L_{st} is replaced with $L_{st}(\tau)$. We must also take into account that now the number of bridges is smaller than n: $n_{br} \sim \psi_{br}n$ since bridges are now formed with low probability $\psi_{br}/(1 + \psi_{br}) \simeq \psi_{br}$, where $\psi_{br} \sim \tau_c/\tau \ll 1$. As a result we get: $R_{st}(\tau) \sim (lL_{st}(\tau))^{1/2} \sim l(l/\Delta)^{2/3}(\tau_c/\tau)^{1/2}$ and

$$n \sim \left(\frac{L}{L_{st}(\tau)}\right)^2 \frac{R_{st}(\tau)^3}{V} \sim \frac{n_l l}{R_{st}(\tau)} \sim n_l\left(\frac{\Delta}{l}\right)^{2/3}\left(\frac{\tau}{\tau_c}\right)^{1/2},$$
$$n_{br} \sim n_l\left(\frac{\Delta}{l}\right)^{2/3}\left(\frac{\tau_c}{\tau}\right)^{1/2} \qquad (140)$$

Eqn (140) are valid as long as $L_{st}(\tau) > l$, that is, $\tau \lesssim \tau^\star \sim (\Delta/l)^{2/3}$ and, in addition, $\tau \gtrsim \tau_c$. The free energy of bridging, $F_{br} \sim -Tn_{br}$ (see eqn (136) and (140)) dominates the repulsion energy F_{rep} (eqn (114)) if

$$\tau < \tau_{gl} \sim (\Delta/l)^{4/3} \qquad (141)$$

Obviously $\tau_c \ll \tau_{gl} \ll \tau^\star$. Thus, we predict that the A/B polymer complex forms a globule at $u < u^\star$ for $0 < \tau \lesssim \tau_{gl}$. Polymer concentration ϕ in the globule can be obtained using the same criterion as before, *i.e.* by demanding that the length fraction of bridges, $n_{br}L_{st}(\tau)/L$, is about 1/2 (that is, it is close to the maximum value). It leads to

$$\phi \sim (\Delta/l)^{8/3}(\tau/\tau_c)^{3/2}, \quad \tau_c \lesssim \tau \lesssim \tau_{gl} \qquad (142)$$

In the above τ-range the volume fraction ϕ is still below the nematic transition threshold, $\phi_{in} \sim 10\Delta/l$; moreover, the third-virial term (due to steric repulsion of polymer segments) remains always negligible here. Note that for $0 < \tau \lesssim \tau_c$ the volume concentration ϕ in the globule is given in eqn (138).

At $\tau > \tau_{gl}$ the bridging attraction is weak, so polymer chains always stay in the coil conformation (in particular, a globular complex is not expected in the case of just 2 chains, A and B, considered above). Turning to the case of a dilute or semidilute binary polymer solution (with stoichiometric A/B composition) we predict that the system should stay homogeneous at $\tau > \tau_{gl}$, but phase separate at lower τ (higher u) if its initial concentration is below the threshold defined in eqn (138) and (142).

Thus, we predict that the chains are not paired in dilute solution at $\tau > \tau_{gl}$ (that is, for low attraction strength, $u < u_1 = u^\star(1 - \tau_{gl})$). The chain gyration radius R_g in this regime is therefore close to that of an ideal WLC, $R_g \approx R_{g0} \sim \sqrt{Ll}$ (for $L \gg l$; the condition $L \lesssim L_m$ is also assumed). At u just above u_1 the bridging attraction leads to globule formation in the regime of extreme dilution. In this case the gyration radius strongly decreases to the globule size which comes from the condition $\phi R_g^3 \sim L\Delta^2$, where ϕ is defined in eqn (142) with $\tau \sim \tau_{gl}$. Hence $R_g \sim L^{1/3}l^{5/9}\Delta^{1/9}$ at $u = u_1 + 0$ (note that here $R_g \ll R_{g0}$ since $L \gg \lambda^\star$). Finally, at $u = u_2 = u^\star(1 + \tau_g)$, where τ_g is defined in eqn (132), the globules get destabilized leading to chain expansion to $R_g \sim \sqrt{2}R_{g0}$, where the factor $\sqrt{2}$ accounts for enhanced rigidity of double-strand (ladder) complexes dominating at $u > u_2$.

D10. Bundle *vs.* elastic beam

Let us return to the regime of strong attraction, $-\tau \gg \tau^\star$. In this case the terminal separation h between WLCs in the double-chain complex is small, $h \ll l$ (more precisely, $h \sim s^{3/2}l^{-1/2}$, where s is the typical loop length, $s \sim 1/\epsilon \sim \lambda^\star/|\tau|$, so that $h \sim l(\tau^\star/|\tau|)^{3/2}$), hence the double-chain can be considered as a fibril with effective Kuhn length $l_2 \simeq 2l_1$ (*cf.* the first term in eqn (4)), where l_1 is Kuhn length of one WLC. Thus, the rigidity is additive here. For a bundle of n chains the result would be $l_n \simeq nl_1$ in the regime $h \ll l$. By contrast, the elastic beam theory applied to bundles predicts a stronger dependence $l_n \sim n^2l_1$ in the limit of strong interactions of constituent chains.[54] The difference comes from the fact that the beam theory

assumes a solid-like bundle with permanent bonds between the chains, while our model allows for a quasi-free gliding of the chains along their contours (due to a quasi-continuous distribution of interacting sites along the chains). The gliding mechanism should involve exchanges between trains and loops (in particular, consumption of some trains by loops and reverse moves) leading to reptation-like dynamics of chain fragments along the bundle.

D11. The role of tails

Returning to adsorption onto a bar: a typical conformation of an adsorbed chain involves many loops and only 2 tails. Just this notion suggests that the contribution of tails in the segmental concentration profile is not large. To neglect the tails we can demand $\epsilon L \gg 1$ (this condition is equivalent to $u/u^\star - 1 \gg \tau_c \sim (\Delta/l)^2$, cf. Section 3.5): in this case the terminal tail/loop length is $s_m \sim 1/\epsilon \ll L$. The adsorbed chain can be roughly considered as a system of blobs (of size s_m for $s_m \gtrsim \lambda^\star/\tau_c$), the number of internal blobs corresponding to loops, $n_{bi} \sim L/s_m \sim \epsilon l \gg 1$, being much larger than just two end-blobs corresponding to tails. The tail contribution can be therefore safely neglected at all scales (up to the terminal distance h from the bar, cf. eqn (55)).

However, even at the critical point $u = u^\star$ ($\tau = 0$) the tail contribution is not so important: in fact, the tail-length (s) distribution is nearly uniform at $\lambda^\star \ll s \ll L$ (cf. point D4), from which we immediately deduce that the mean masses of all loops and all tails are comparable. More precisely, the tail-length distribution at $\tau = 0$ can be generated just by randomly choosing two points (A and B) on the WLC of length L. (This procedure comes from the notion that at $\tau = 0$ the statistical weight of a tail is independent of its length, and the same is true for the middle segment AB involving loops and trains.) As a result we find that the mean length of each tail, L_t, is $L_t \approx L/3$, which is also nearly equal to the length of all loops (corresponding to the segment AB; note that the contribution of trains to its length is negligible if $L \gg L_{tt}$, cf. point D5).†††

Turning to the distribution of the loop and tail segments around the bar, note that the terminal distance h is defined by the coil size at $\tau = 0$, $h \sim R_{coil} \sim \sqrt{Ll}$, so h is large for long chains and most of the loop and tail segments are located at $r \sim h$. The distribution of loop segments $c_l(r)$ is defined in eqn (45) (the tail contribution is neglected in this equation). As for segments of the tails, their distribution $c_t(r)$ (with scaling accuracy) is similar to the free-end distribution given in eqn (94): $c_t(r) \propto \psi'(r)$, as follows from the ideal WLC statistics of the tails (also note that it is long tails of length $s \sim L$ that provide the dominant contribution to $c_t(r)$ for all $r \lesssim h$). Recalling that loop and tail masses are comparable we find that:

$$c_l(r) \sim c_t(r) \quad \text{for } r \sim h$$

Noting also that $c_l(r)$ increases faster than $c_t(r)$ as r is decreased in the region $r \ll h$ (cf. eqn (45) and (94)), we can conclude that

$c_l(r) \gg c_t(r)$ in this region, so tails are subdominant at $\tau = 0$ in the whole range of major interest, $r \ll h$.

5 Summary and conclusions

We theoretically studied association of two semiflexible worm-like chains (A and B) driven by mutual short-range attraction of their segments (the interaction energy vanishes at $r > \Delta$) in the case of high chain stiffness, when the chain persistence length $l_p = l/2$ is much longer than the interaction range Δ. The chains tend to align parallel to each other forming a double-strand complex due to their side-to-side attraction (defined by the parameter u equal to the depth of the interaction potential well divided by the thermal energy T, cf. Fig. 3a). It is shown that the local structure of such complex (at length scales $r \ll l_p$) is identical to that of a semiflexible WLC (chain A* with renormalized stiffness defined in eqn (106)) adsorbed onto a straight bar (replacing the second chain B).

We found that the critical strength of attraction, $u = u^\star$, corresponding to the adsorption threshold (such that the A*-chain becomes trapped in the vicinity of the bar beyond the threshold, at $u > u^\star$) scales as $u^\star \sim (\Delta^2 l)^{-1/3}$ (see eqn (31)). A similar $u^\star$ was predicted for adsorption of a WLC onto a solid surface or membrane.[5–7,49]

At $u = u^\star$ the adsorbed structure involves 3 regions: the contact region (at the distance $r < \Delta$ from the bar), the proximal cylindrical layer (at $\Delta < r \ll l$) and the distal corona layer ($r \gg l$). At the critical point the contact layer consists of train segments (of typical length $s \sim \lambda^\star$, $\lambda^\star \sim (l\Delta^2)^{1/3}$) interacting with the bar and aligned parallel to it: the typical angle between a train and the bar is $\theta \sim \Delta/\lambda^\star \sim (\Delta/l)^{1/3}$. Using a scaling argument we established that the proximal layer shows a fractal structure of aligned loops (connecting the trains) implying an algebraic decay of polymer concentration, $c(r) \propto r^{-10/3}$ there. Moreover, using the transfer matrix approach (see eqn (20)) we obtained the orientational distribution of A-chain end segments in the proximal layer: it follows a universal law in terms of the reduced variables η, ξ defined with the r-dependent reference (typical) tilt angle with respect to the bar, $\Theta(r/l) = (r/l)^{1/3}$ (cf. eqn (17) and (19)). The asymptotically exact orientational distribution profiles are shown in Fig. 4. As for the distal layer, it consists of long 'isotropic' loops characterized by another self-similar length distribution (cp. eqn (78) and (79) for $\epsilon = 0$).

Above the critical threshold, at $u > u^\star$, the polymer gets trapped by the bar. Depending on the attraction strength u the polymer mass is then dominated by either long loops (for $u/u^\star - 1 \lesssim (\Delta/l)^2$) or by the shortest loops and trains (at $u/u^\star - 1 \gg (\Delta/l)^2 \ln(L/L_{st})$), where $L_{st} \sim l(l/\Delta)^{4/3}$ is the typical supertrain length (see Fig. 6b and c). The loops of intermediate length s ($\lambda^\star \ll s \ll l$) are never dominant, i.e. the loops are segregated spatially in two classes according to their sizes. This effect is reminiscent of segregation of chromatin loops between compartments in folded chromosomes.[55]

The net free energy gain on adsorption of a single WLC of length L, εLT, becomes positive at $u > u^\star$. At small $u/u^\star - 1$ it

---

††† A more general argument to obtain the tail-length distribution at $u = u^\star$ is given in Section 7.3 of ref. 7.
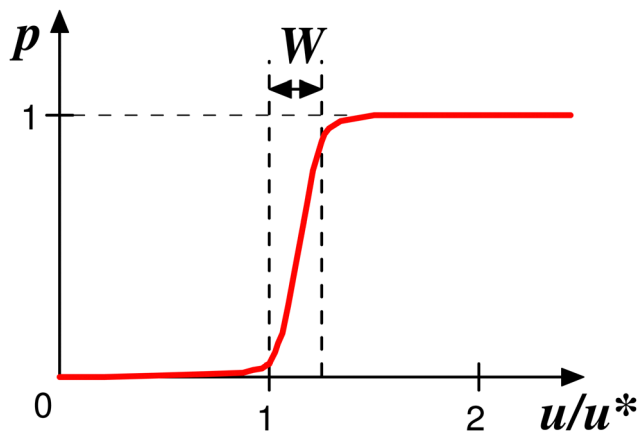
Fig. 11 The fraction $p = p(\Delta, \infty)$, eqn (73), of monomers interacting with the bar *vs.* the reduced attraction strength, u/u^*. The transition width is $W \sim \tau_c \sim (\Delta/l)^2$. The steepness is $S = 1/W$.

increases in an exponential fashion $\varepsilon \propto \exp(S(u/u^* - 1))$ with high steepness $S \sim (l/\Delta)^2$, *cf.* eqn (67). The fraction p of train sections increases in parallel, it changes from almost zero at $u = u^*$ to $p \sim 1$ in a narrow region $0 < u/u^* - 1 \lesssim (\Delta/l)^2$ (see Fig. 11 and eqn (73)). Therefore, although the condensation of the A^*-chain is continuous, it becomes similar to a first-order phase transition for high stiffness, $l \gg \Delta$. Similar p-jumps (but with lower steepness) were predicted for adsorption of semiflexible chains onto solid surfaces ($S \sim (l/\Delta)^{4/3}$) and permeable membranes ($S \sim (l/\Delta)^{2/3}$).[6,7] A qualitatively similar 'rounded phase transition' was also predicted for linker-induced aggregation of two semiflexible polyelectrolytes.[31] Furthermore, we established that the distal layer is suppressed at $u/u^* - 1 \gtrsim (\Delta/l)^{2/3} = \tau^*$. A further increase of the interaction parameter u leads to a shrinkage of the proximal region whose cut-off radius decreases as $\Delta/(u/u^* - 1)^{3/2}$ (see eqn (71)).

Replacing the bar with the second WLC we analysed the equilibrium structure of double-strand complexes and the properties of (dilute or semidilute) binary solutions of the WLCs. In a dilute binary solution at stoichiometric conditions the chains tend to form complexes if monomer attraction is strong enough, $u > u^*$. Moreover, if $u/u^* - 1 \gg \tau^*$, the paired chains are always nearly parallel to each other in a double-strand complex (*cf.* Fig. 9a) and their separation r does not exceed l being typically very short, $r \sim \Delta$. The double-strand chain remains in the coil state if all attractive interactions (bonds) are already saturated in the paired structure (*cf.* ladder segment in Fig. 1c). However, at higher concentrations (in the semidilute regime, $c > c^*$) branching of double-chains by strand exchange (*cf.* Fig. 8 and Discussion point D7) becomes important leading to gelation of the system (*cf.* Fig. 9f) above some concentration c_g defined in eqn (116). We also found that strand exchange becomes even more important at weaker attraction, $u/u^* - 1 < \tau^*$ (*cf.* Fig. 9d and e), leading to a collapse of double chains already in the dilute solution regime if $u/u^* - 1 \lesssim (\Delta/l)^{4/3}$ (*cf.* eqn (132)). More generally we established that double-strand complexes form globules or phase separate (in dilute or semidilute regimes) within a finite range of attraction strength u around the critical point:

$$- (\Delta/l)^{4/3} \lesssim u/u^* - 1 \lesssim (\Delta/l)^{4/3} \qquad (143)$$

(see Discussion points D8, D9). Thus, as u increases the polymer component is predicted to first precipitate at $u > u_1$ and then redissolve at $u > u_2$, where u_1, u_2 can be deduced from eqn (143). Such a reentrant transition to the solution phase (induced by an increase of the attraction strength u) is reminiscent of redissolution of aggregated semirigid macromolecules (like DNA and F-actin) in aqueous solution upon adding high amounts of multivalent ions which normally promote interchain attraction.[56,57]

The side-to-side attraction of stiff polymer chains in solution can generally lead to their precipitation due to formation of a dense phase with chains aligned nearly parallel to each other. However, in some cases such transition does not occur directly, but rather is preempted by formation of finite bundles of aligned chains. The simplest bundle is a double-chain considered in the present paper. Such pairing is expected, for example, if the attraction is provided by transient saturating bonds,[58] like H-bonds or other directional interactions. The theory of double-chain complexes emerging as solvent quality is decreased and their structural properties elucidated here can provide a useful basis for correct interpretation of scattering experiments on WLC polymer systems.

We thus provide a theoretical framework to study lateral association of dissolved semiflexible polymers with short-range attractive interactions. The obtained results can be applied to study aggregation, bundling and network formation in solutions of synthetic polymers and biopolymers with rigid backbone (like DNA, F-actin[59] and other protein bio-filaments).

Conflicts of interest

There are no conflicts of interest to declare.

Acknowledgements

References

1 L. Bouteiller, O. Colombani, F. Lortie and P. Terech, Thickness transition of a rigid supramolecular polymer, *JACS*, 2005, **127**, 8893–8898.

2 F. Lin, *et al.*, The construction of rigid supramolecular polymers, *Chem. Commun.*, 2014, **50**, 7982–7985.

3 I. A. Nyrkova and A. N. Semenov, *Eur. Phys. J. E*, 2018, **41**, 103.

4 E. B. Zhulina, A. A. Gorbunov, T. M. Birshtein and A. M. Skvortsov, *Biopolymers*, 1982, **21**, 1021.

5 A. C. Maggs, D. A. Huse and S. Leibler, Unbinding Transitions of Semi-flexible Polymers, *Europhys. Lett.*, 1989, **8**, 615–620.

6 A. N. Semenov, *Eur. Phys. J. E*, 2002, **9**, 353–363.

7 A. N. Semenov and I. A. Nyrkova, *Polymers*, 2023, **15**, 35.

8 J. Baschnagel, H. Meyer, J. Wittmer, I. Kulić, H. Mohrbach, F. Ziebert, G. M. Nam, N. K. Lee and A. Johner, Semiflexible Chains at Surfaces: Worm-Like Chains and beyond, *Polymers*, 2016, **8**, 286.

9 I. Nyrkova, E. Moulin, J. J. Armao IV, M. Maaloum, B. Heinrich, M. Rawiso, F. Niess, J.-J. Cid, N. Jouault, E. Buhler, A. N. Semenov and N. Giuseppone, *ACS Nano*, 2014, **8**, 10111.

10 J. J. Armao IV, I. Nyrkova, G. Fuks, A. Osypenko, M. Maaloum, E. Moulin, R. Arenal, O. Gavat, A. Semenov and N. Giuseppone, *J. Am. Chem. Soc.*, 2017, **139**, 2345.

11 A. Aggeli, M. Bell and N. Boden, *et al.*, *Nature*, 1997, **386**, 259.

12 I. A. Nyrkova, A. N. Semenov, A. Aggeli and N. Boden, *Eur. Phys. J. B*, 2000, **17**, 481.

13 A. Aggeli, M. Bell, N. Boden, J. N. Keen, T. C. B. McLeish, I. Nyrkova, S. E. Radford and A. Semenov, *J. Mater. Chem.*, 1997, **7**, 1135.

14 A. Aggeli, M. Bell, N. Boden, R. Harding, T. C. B. McLeish, I. Nyrkova, S. E. Radford and A. Semenov, *Biochemist*, 2000, **22**, 10.

15 J. Schnauss, T. Handler and J. A. Kas, Semiflexible Biopolymers in Bundled Arrangements, *Polymers*, 2016, **8**, 274.

16 W. Janke, Computer Simulation Studies of Polymer Adsorption and Aggregation: From Flexible to Stiff, *Phys. Proc.*, 2015, **68**, 69–79.

17 V. A. Kabanov, A. B. Zezin, V. A. Izumrudov, T. K. Bronich and K. N. Bakeev, *Makromol. Chem.*, 1985, **13**, 137.

18 V. A. Kabanov, *Russ. Chem. Rev.*, 2005, **74**, 3.

19 V. A. Kabanov, Fundamentals of Polyelectrolyte Complexes in Solution and the Bulk, in *Multilayer Thin Films; Sequential Assembly of Nanocomposite Materials*, ed. G. Decher and J. B. Schlenoff, Wiley, New York, 2003.

20 K. N. Bakeev, V. A. Izumrudov, S. I. Kuchanov, A. B. Zezin and V. A. Kabanov, *Macromolecules*, 1992, **25**, 4249.

21 V. A. Kabanov, *Polym. Sci.*, 1993, **36**, 143.

22 A. V. Kabanov, T. K. Bronich, V. A. Kabanov, K. Yu and A. Eisenberg, *Macromolecules*, 1996, **29**, 6797.

23 V. A. Kabanov, A. B. Zezin, V. B. Rogacheva, Z. G. Gulyaeva, M. F. Zansochova, J. G. H. Joosten and J. Brackman, *Macromolecules*, 1999, **32**, 1904.

24 C. E. Sing and S. L. Perry, Recent Progress in the Science of Complex Coacervation, *Soft Matter*, 2020, **16**, 2885–2914.

25 A. V. Subbotin and A. N. Semenov, The Structure of Polyelectrolyte Complex Coacervates and Multilayers, *Macromolecules*, 2021, **54**, 1314.

26 S. L. Dakhara and C. C. Anajwala, Polyelectrolyte Complex: A Pharmaceutical Review, *Systematic Rev. Pharm.*, 2010, **1**, 121–127.

27 B. Philipp, H. Doutzenberg, K. J. Linow, J. Koetz and W. Dowydoff, Polyelectrolyte complexes – recent development and open problems, *Prog. Polym. Sci.*, 1989, **14**, 91.

28 V. A. Izumrudov, A. B. Zezin and V. A. Kabanov, *Russ. Chem. Rev.*, 1991, **60**, 792.

29 A. A. Lazutin, A. N. Semenov and V. V. Vasilevskaya, Polyelectrolyte Complexes Consisting of Macromolecules With Varied Stiffness: Computer Simulation, *Macromol. Theory Simul.*, 2012, **21**, 328–339.

30 S. Adhikari, M. A. Leaf and M. Muthukumar, Polyelectrolyte complex coacervation by electrostatic dipolar interactions, *J. Chem. Phys.*, 2018, **149**, 163308.

31 I. Borukhov, K.-C. Lee, R. F. Bruinsma, W. M. Gelbart, A. J. Liu and M. J. Stevens, Association of two semiflexible polyelectrolytes by interchain linkers: Theory and simulations, *J. Chem. Phys.*, 2002, **117**, 462.

32 S. P. O. Danielsen, A. N. Semenov and M. Rubinstein, Phase Separation and Gelation in Solutions and Blends of Heteroassociative Polymers, *Macromolecules*, 2023, **56**, 5661–5677.

33 P. Cordier, F. Tournilhac, C. Soulie-Ziakovic and L. Leibler, Self-Healing and Thermoreversible Rubber from Supramolecular Assembly, *Nature*, 2008, **451**, 977–980.

34 E. B. Stukalin, L. H. Cai, N. A. Kumar, L. Leibler and M. Rubinstein, Self-Healing of Unentangled Polymer Networks with Reversible Bonds, *Macromolecules*, 2013, **46**, 7525–7541.

35 M. A. C. Stuart, W. T. S. Huck, J. Genzer, M. Muller, C. Ober, M. Stamm, G. B. Sukhorukov, I. Szleifer, V. V. Tsukruk, M. Urban, F. Winnik, S. Zauscher, I. Luzinov and S. Minko, Emerging Applications of Stimuli-Responsive Polymer Materials, *Nat. Mater.*, 2010, **9**, 101–113.

36 O. Kratky and G. Porod, Röntgenuntersuchung gelöster Fadenmoleküle, *Rec. Trav. Chim.*, 1949, **68**, 1106.

37 B. Li and S. M. Abel, Shaping membrane vesicles by adsorption of a semiflexible polymer, *Soft Matter*, 2018, **14**, 185–193.

38 F. Meng and E. M. Terentjev, Theory of Semiflexible Filaments and Networks, *Polymers*, 2017, **9**, 52.

39 P. G. De Gennes, *Scaling Concepts in Polymer Physics*, Cornell Univ. Press, Ithaca, 1985.

40 I. Murakami, *Polym. J.*, 1976, **8**, 150.

41 A. A. Gorbunov, E. B. Zhulina and A. M. Skvortsov, *Polymer*, 1982, **23**, 1133.

42 A. Grosberg and A. Khokhlov, *Statistical Physics of Macromolecules*, American Institute of Physics, New York, 1994.

43 S. F. Edwards, The statistical mechanics of polymers with excluded volume, *Proc. Phys. Soc.*, 1965, **85**, 613.

44 A. Y. Grosberg, On Some Possible Conformational States of Homogeneous Elastic Polymer Chain, *Biofizika*, 1979, **24**, 30–36.

45 P. Agarwal, J. Choi and S. Jain, Extended Hypergeometric Functions of Two and Three Variables, *Commun. Korean Math. Soc.*, 2015, **30**, 403–414.

46 K. Binder, Critical Behaviour at Surfaces, in *Phase Transitions and Critical Phenomena*, ed. C. Domb and J. L. Lebowitz, Academic Press, London, 1983, vol. 8, p. 1.

47 M. E. Fisher, Walks, walls, wetting, and melting, *J. Stat. Phys.*, 1984, **34**, 667–729.

48 E. Eisenriegler, *Polymers Near Surfaces*, World Scientific, Singapore, 1993.

49 A. Milchev and K. Binder, How does stiffness of polymer chains affect their adsorption transition?, *J. Chem. Phys.*, 2020, **152**, 064901.

50 L. D. Landau and E. M. Lifshitz, *Statistical Physics*, Pergamon Press, Oxford, 1998.

51 A. N. Semenov and M. Rubinstein, Thermoreversible Gelation in Solutions of Associative Polymers. 1. Statics, *Macromolecules*, 1998, **31**, 1373–1385.

52 P. J. Flory, *Principles of Polymer Chemistry*, Cornell Univ. Press, Ithaca, 1953.

53 A. N. Semenov and A. R. Khokhlov, Statistical physics of liquid-crystalline polymers, *Sov. Phys. Usp.*, 1988, **31**, 988–1014.

54 C. Heussinger, F. Schüller and E. Frey, *Phys. Rev. E: Stat., Nonlinear, Soft Matter Phys.*, 2010, **81**, 021904.

55 W. J. Xie, L. Meng, S. Liu, L. Zhang, X. Cai and Y. Q. Gao, Structural Modeling of Chromatin Integrates Genome Features and Reveals Chromosome Folding Principle, *Sci. Rep.*, 2017, **7**, 2818.

56 J. Pelta, F. Livolant and J.-L. Sikorav, *J. Biol. Chem.*, 1996, **271**, 5656; E. Raspaud, M. Olvera de la Cruz, J.-L. Sikorav and F. Livolant, *Biophys. J.*, 1998, **74**, 381; E. Raspaud, I. Chaperon, A. Leforestier and F. Livolant, *Biophys. J.*, 1999, **77**, 1547.

57 J. X. Tang and P. A. Janmey, *J. Biol. Chem.*, 1996, **271**, 8556; J. X. Tang, S. Wong, P. T. Tran and P. A. Janmey, *Ber. Bunsenges. Phys. Chem.*, 1996, **100**, 796.

58 I. M. Lifshitz, A. Y. Grosberg and A. R. Khokhlov, *Sov. Phys. JETP*, 1976, **44**, 855.

59 K. R. Ayscough, In vivo functions of actin-binding proteins, *Curr. Opin. Cell Biol.*, 1998, **10**, 102.